

Molecular Crystals and Liquid Crystals

Publication details, including instructions for authors and subscription information:

<http://www.tandfonline.com/loi/gmcl16>

The Effect on Mesomorphic Properties of Substituting a Sulfur for the Ether Oxygen Atom in the Ester Linkage of 4-Alkylphenyl-4'-Alkyl or Alkoxybenzoates

Mary E. Neubert^a, R. E. Cline^a, M. J. Zawaski^a
^c, P. J. Wildman^a & Arun Ekachai^{b d}

^a Liquid Crystal Institute, Kent State University, Kent, Ohio, 44242

^b Liquid Crystal Institute and Department of Physics

^c Carlon, An Indian Head Company, Aurora, Ohio

^d Department of Physics, Prince of Songkla University, Haad Yai, Thailand

Version of record first published: 20 Apr 2011.

To cite this article: Mary E. Neubert, R. E. Cline, M. J. Zawaski, P. J. Wildman & Arun Ekachai (1981): The Effect on Mesomorphic Properties of Substituting a Sulfur for the Ether Oxygen Atom in the Ester Linkage of 4-Alkylphenyl-4'-Alkyl or Alkoxybenzoates, *Molecular Crystals and Liquid Crystals*, 76:1-2, 43-77

To link to this article: <http://dx.doi.org/10.1080/00268948108074675>

Full terms and conditions of use: <http://www.tandfonline.com/page/terms-and-conditions>

This article may be used for research, teaching, and private study purposes. Any substantial or systematic reproduction, redistribution, reselling, loan, sub-licensing, systematic supply, or distribution in any form to anyone is expressly forbidden.

The publisher does not give any warranty express or implied or make any representation that the contents will be complete or accurate or up to date. The accuracy of any instructions, formulae, and drug doses should be independently verified with primary sources. The publisher shall not be liable for any loss, actions, claims, proceedings, demand, or costs or damages whatsoever or howsoever caused arising directly or indirectly in connection with or arising out of the use of this material.

The Effect on Mesomorphic Properties of Substituting a Sulfur for the Ether Oxygen Atom in the Ester Linkage of 4-Alkylphenyl-4'-Alkyl or Alkoxybenzoates†

MARY E. NEUBERT, R. E. CLINE, M. J. ZAWASKI‡ and P. J. WILDMAN

Liquid Crystal Institute, Kent State University, Kent, Ohio 44242

and

ARUN EKACHAI§

Liquid Crystal Institute and Department of Physics

(Received October 24, 1980)

A variety of homologs of 4-alkylbenzenethio-4'-alkyl or alkoxybenzoates in which the 4'-alkoxy group is C₇-C₁₄, the 4'-alkyl group is C₇-C₁₂ and the 4-alkyl group is C₃-C₈ or C₁₀ were prepared and their mesomorphic properties studied by microscopy, DSC and X-ray diffraction. A comparison is made of the mesomorphic properties in the thio- and oxy-esters and the effect on mesomorphic properties of replacing the ether oxygen atom in the ester linkage with a sulfur atom. The types of smectic phases observed are discussed; two apparently new biaxial smectic phases were found in the alkoxy-alkyl series. Relationships between mesomorphic and thermodynamic properties with molecular structure are discussed.

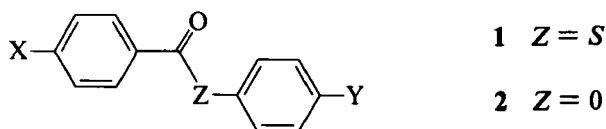
INTRODUCTION

We first became interested in studying the mesomorphic properties of the thioesters 1

† Presented in part at the Ninth Northeast Regional American Chemical Society Meeting, Syracuse, New York, 1979 and at the 8th International Liquid Crystal Conference, Kyoto, Japan, 1980, abst. No. E4.

‡ Present address: Carlon, An Indian Head Company, Aurora, Ohio.

§ Present address: Department of Physics, Prince of Songkla University, Haad Yai, Thailand.



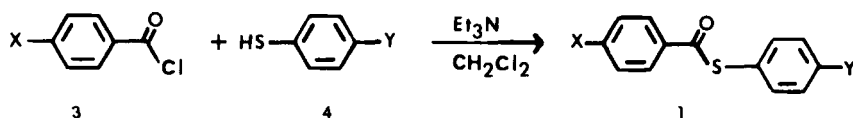
when earlier work by Reynolds, *et al.*¹ indicated that several of these compounds showed types of mesophase transitions which would be useful in Johnson's phase transition studies of mixtures.^{2,3} Their enhanced stability over that for the anils made them attractive for physical studies as well. However, we were also interested in the effect on mesomorphic properties of substituting the ether oxygen atom in the central linkage of the oxy-esters **2** with a sulfur atom. Preliminary data suggested that this structural change favored the formation of smectic phases. This was of interest to us in our continuing studies of the relationship between smectic properties and molecular structure.^{4,5} Thus, we prepared a variety of homologs of these thioesters in which *X* is a C₇–C₁₄ alkoxy or C₇–C₁₂ alkyl group and *Y* = C₃–C₈ or C₁₀ alkyl group.

Various thioesters of this type have been reported^{1,6–8} but the goal in these studies was to design new nematic mesogens for use in electronic display devices. Consequently, most of the compounds studied contained shorter alkyl chains which do not favor formation of smectic phases.

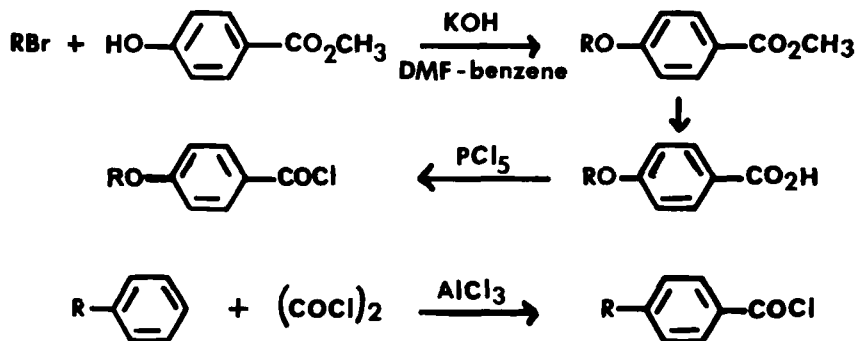
Reynolds developed an abbreviated nomenclature for these thioesters in which the number of carbon atoms in *X* is given first followed by *S* indicating a thioester (i.e. $Z = S$) and then the number of carbon atoms in *Y* with the structure written as in **1**. A line drawn over one of these numbers indicates that the alkyl chain is attached to an oxygen atom. Thus, when $X = C_8H_{17}O$ and $Y = C_5H_{11}$, the designation is $\overline{8}S5$ and when $X = C_8H_{17}$, it is $8S5$.

SYNTHESIS

Most of these thioesters were prepared by esterification of the benzoyl chloride **3** with the 4-alkylbenzenethiol **4** using triethylamine as the base in CH₂Cl₂ (scheme 1). Crude yields ranged from 90–100%. Purification was usually by recrystallization from absolute ethanol although with longer chain homologs, ethyl acetate or chloroform had to be added to keep the thioesters in solution during filtrations to remove insoluble impurities. DSC proved to be the most useful method for detecting impurities.



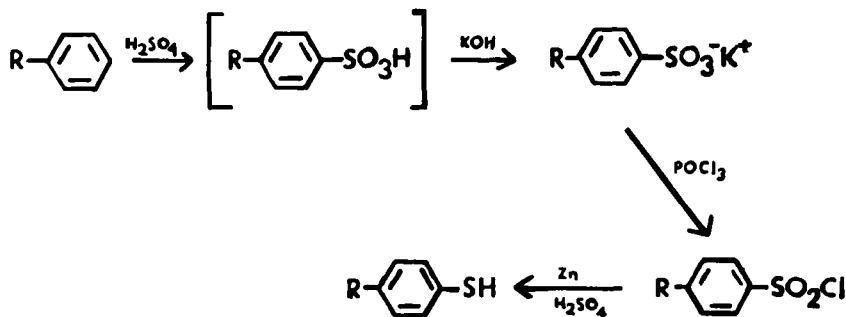
SCHEME 1



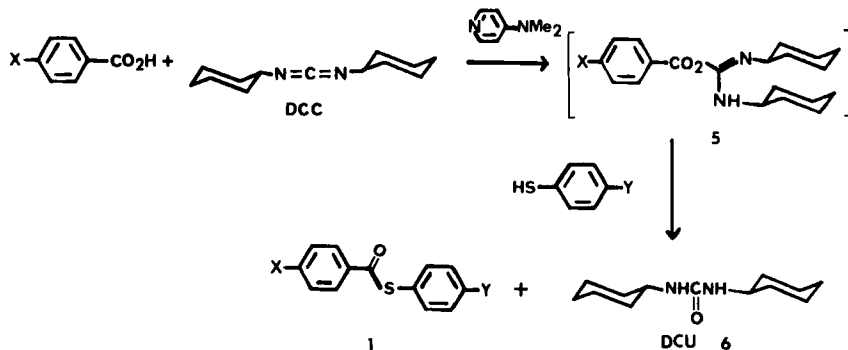
SCHEME 2

The benzoyl chlorides were prepared by the reactions shown in scheme 2 and discussed extensively in Refs. 9 and 10. In the preparation of 4-alkoxybenzoic acids (Ref. 9), we sometimes had to eliminate the basic extraction in the isolation of the methyl ester of the longer chain homologs because of the difficulty with emulsions and also, the ether extraction in the hydrolysis step because of the low solubility of these homologs in ether. Yields of 4-alkylbenzoyl chlorides were found to be lower on days when the humidity was high emphasizing that care must be used in the synthesis of these compounds to use anhydrous conditions. 4-Alkoxybenzoic acids through C_{10} (Frinton Laboratories) and 4-alkylbenzoyl chlorides (C_1 , C_3 – C_8 , C_{10} , Eastman Kodak Co.) are now commercially available. 4-Alkylbenzenethiols were prepared according to scheme 3 and as detailed in Ref. 11. Care should be taken in handling these thiols to avoid skin contact since they cause skin irritation in some people.

Since the benzoyl chlorides with alkyl chain lengths $>\text{C}_{10}$ were difficult to purify, we decided to try a modified carbodiimide reaction^{12,13} (scheme 4) which converts the benzoic acid *in situ* to the reactive intermediate 5 which then reacts with the thiol in the presence of a base to give the thioester in crude



SCHEME 3



yields of $\sim 80\%$ and *N,N'*-dicyclohexylurea **6** as a by-product. Typical examples of experimental procedures for both methods for preparing the thioesters are given in the experimental section.

MESOMORPHIC PROPERTIES

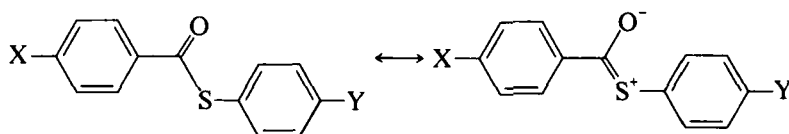
Transition temperatures (obtained from microscopy studies) for the alkoxy-alkyl thioesters prepared are given in Table I. Values for the dialkyl series are presented in Table II.

A comparison of the melting temperatures for the thioesters **1** ($X = RO$, $Y = C_5$) with those for the corresponding oxy-esters **2** presented in Table III shows similar melting temperatures for both series. However, a comparison of the clearing temperatures (Table IV) shows that the thioesters have values of $\sim 20^\circ$ higher than those for the oxy-esters. This gives a wider temperature range over which enantiotropic mesophases can occur.

The effect of replacing the oxygen atom with a sulfur atom in the oxy-esters **2** has on the type of mesophases observed is shown in Table V. When X is an alkoxy group in the oxy-esters only smectic A and nematic phases are observed whereas in the thioesters a wide variety of smectic phases in various combinations occur in addition to the nematic phase. When X is an alkyl group, the oxy-esters show either short range nematic phases or no mesomorphic properties at all while the thioesters show nematic, smectics A and B phases.

A comparison of the structural features for these esters (Table VI) provides a possible explanation for this difference. Although the C—S—C bond angle is smaller than the C—O—C angle, the carbon-sulfur bond is longer than the carbon-oxygen bond. This gives the overall effect of increasing the planarity of the molecules which increases the lateral forces and favors formation of

smectic phases. The larger dipole moment observed for diphenyl sulfide than that for diphenyl ether, a relationship expected also in the esters, would favor formation of smectic phases. The smaller electronegativity for the sulfur atom compared to that for the oxygen atom would increase the resonance in these thioesters in the following manner:



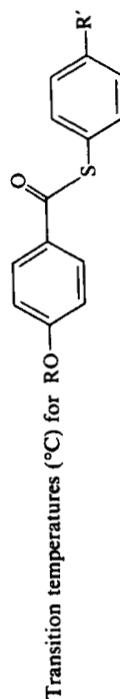
The effect of this increased resonance is observed in the shift of the carbonyl group in the infrared spectrum to a longer wavelength for the thioesters and would also favor the formation of smectic phases.

A plot of the transition temperatures as a function of alkyl chain length for a series of thioesters in which the alkyl group is kept constant (C_5) while the alkoxy group is varied (Figure 1) shows a typical odd-even alternating curve for nematic-to-isotropic transitions with the nematic phase decreasing in length until it disappears at $R = C_{12}$. Below the nematic phase occurs a smectic *A* phase with increasing phase length as the nematic phase length decreases. It is obvious that the smectic *A* phase will appear in homologs with longer than C_{14} alkoxy groups but will decrease in length with the increasing phase length of the smectic *B* phase introduced at $R = C_{12}$. When $R < C_{13}$, a smectic *C* phase, either monotropic or enantiotropic, occurs below the smectic *A* phase. A monotropic biaxial phase, designated smectic *Y*, which shows a mosaic texture and a non-centered biaxial cross in microscopy studies and a smectic *B* type structure by powdered X-ray diffraction studies¹⁸ occurs below the smectic *A* phase when $R < C_{12}$. This phase is replaced by a uniaxial smectic *B* plus smectic *X*† combination at longer alkyl chain lengths. This smectic *X* phase is also a biaxial, smectic *B* type phase but shows both fan and mosaic textures and a centered biaxial cross. The smectic *B* to smectic *X* transition appears to be second order as shown by the subtle, continuous changes observed in the microscopic texture, X-ray diffraction studies and the small thermal heat change observed by DSC. Johnson has confirmed this second order nature by calorimetric studies.¹⁹

A similar plot for a series in which the alkoxy group is kept constant (C_8) while the alkyl group is varied (Figure 2) shows the weaker effect that changing the length of the alkyl group on the thiol end of the molecule has on the

† The structure of the smectic *X* phase has been discussed by A. de Vries at the International Conference on Liquid Crystals at Bangalore, India, 1979 and the 8th International Liquid Crystal Conference in Kyoto, Japan, 1980. We have retained his designation for this phase to avoid confusion. See reference 18a for more details.

TABLE I



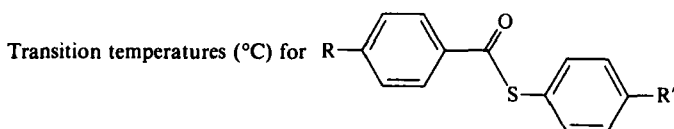
R'	R	C ^a	S _T	S _X	S _B	S _C	S _A	N	I _S
C ₆	C ₆	22	—	—	—	—	—	58.0–59.0	85.9
C ₅	C ₇	22.1	—	—	—	(36.8–36.9) ^b	—	53.4–54.6 ^c	82.9
C ₅	C ₈	19.4	—	—	—	(56.0–56.3)	—	62.7–63.5	86.5
C ₅	C ₉	37.4	(31.1–31.3)	—	—	61.5–62.5 ^a	58.0–58.6	72.6	84.4–84.6
C ₅	C ₁₀	39.3	(39.0–39.2)	—	—	59.7–60.3	62.5–62.7	79.5–79.6	85.4–85.6
C ₅	C ₁₁	27.5	(47.4–47.9)	—	—	62.1–62.5	64.2–64.8	83–83.6	84.7–85.2
C ₅	C ₁₂	27.4	(54.3–54.5)	—	—	60.4–62.4 ^d	61.2–61.4	—	86.2–86.7
C ₅	C ₁₃	31.1	—	(56.7)	(60.0)	—	64.2–64.3	—	87.0–87.2
C ₅	C ₁₄	28.1	—	(61.3–62.5)	62.5–63.1	—	68.3	—	87.9–88.1
C ₆	C ₇	30.6	—	(62.6–63.0)	64.3–64.7	—	—	—	79.0–79.1
C ₆	C ₈	33.2	—	—	—	(45.9)	—	59.4–60.2	83.2
C ₆	C ₉	41.2	(33.8–34.0)	—	—	56.4–57.3	58.4–59.1	68.1	83.6–83.7
C ₆	C ₁₀	30.1	(52.4–52.7)	—	—	(63.3–64.1)	70.8–71.2	81.4–82.2	79.0–83.6 ^e
C ₆	C ₁₂	34.8	(59.0–59.6)	—	—	65.4–66.4	68.2	—	86.3–86.7
C ₇	C ₁₄	28.7	67.0–67.1	—	—	70.4–70.6	74.8–75.0	—	83.2–83.3
C ₇	C ₈	16.5	—	—	—	(44.3)	—	55.0–55.6	86.7
C ₇	C ₉	17.8	(30.9–31.0)	—	—	53.6–54.1	63.2–63.4	69.9–70.2	84.6–84.8
C ₇	C ₁₀	31.3	—	(~36.5)	(41.1–41.3)	56.0–58.0	69.5–69.8	76.9–77.0	86.5–86.7
C ₇	C ₁₁	39.1	—	(45.8)	(54.5–54.8)	59.8–61.6	74.4–74.8	84.2–84.3	86.3–86.7
C ₇	C ₁₂	39.6	—	(55.2)	(60.2–60.5)	67.5–69.1	78.3–78.5	—	88.3–88.6
C ₇	C ₁₄	37.6	—	(63.1)	(67.4–67.8)	67.0–68.9	80.3–80.9	—	89.4–89.7
C ₈	C ₇	31.3	—	(68.4–69.4) ^f	68.4–69.2	74.3–75.2	79.6–80.3	58.5–59.1	81.1–81.2

TABLE I (continued)

C ₈	C ₈	22.0	—	(~26)	(34.9)	55.1-56.0	63.5-63.8	74.1	85.0-85.1
C ₈	C ₁₀	33.9	—	(37.8-41.8)	56.0-56.7	65.0-65.3	74.4-74.5	83.8-84.5	84.8-85.9
C ₈	C ₁₁	38.1	—	(55.3-60.0)	(62.6-62.7)	72.0-74.2	81.3-81.4	—	86.0-86.3
C ₈	C ₁₂	43.5	—	(66.2-67.4)	(69.0-70.0)	71.6-73.2	83.1-84.6	—	87.9-88.1
C ₈	C ₁₄	39.7	—	(74.6-75.4)	—	76.0-76.3	85.0-85.9	—	87.9-88.4
C ₁₀	C ₇	43.2	—	—	—	(56.0)	—	65.2-65.8	80.1-80.2
C ₁₀	C ₈	27.6	—	—	(38.9-39.0)	59.9-60.6	65.1	77.6	84.2
C ₁₀	C ₁₀	30.8	—	—	(62.7-62.8)	65.6-66.3	77.8-79.6	—	86.6-86.7
C ₁₀	C ₁₂	46.2	—	(63.5-64.9)	(74.6)	74.8-75.7	87.8	—	88.0-89.0
C ₁₀	C ₁₄	55.1	—	79.0-81.5 ^g	—	81.5-81.6	—	—	88.9-89.7
C ₁₂	C ₈	39.5	—	—	(43.1-43.4)	(62.8-63.1)	64.2-65.5	78.7	82.4-82.6

^a Crystallization temperature at a cooling rate of 2°/min.^b () indicates a monotropic transition.^c A crystal-to-crystal transition at 51.0-51.2° seems to precede the crystal-to-nematic transition.^d This is a C → S_CA transition. The S_C → S_A transition temperature was obtained by cooling the smectic A to the smectic C phase and reheating.^e The range of this transition was not narrowed by further purification of the sample. The wide range may be due to the tendency of the fan texture to convert to a homeotropic one near the S_A → I transition.^f The transition temperature given for the S_B phase was obtained by heating a crystallized sample and represents the melting point. The transition temperature given for the S_γ phase was obtained by observing the uniaxial cross in the S_B phase converting to a biaxial cross in the S_γ phase on cooling and then reheating until the cross reappeared. Since this temperature is the same as that observed for the melting point, the melting temperature could be a C → S_γB although in all other cases the S_γ appears to be a monotropic.^g Some change occurs ~51°, possible a crystal-to-crystal change.

TABLE II



R'	R	C^1	S_B	S_A	N	I_S
C_5	C_6	26.7	—	—	(44.3–44.5) ²	47.1–47.5
C_5	C_8	26.2	—	—	39.4–40.9	49.0–49.5
C_5	C_9	10.8	(29.2–29.7)	(34.1)	38.1–39.4	55.6–55.7
C_5	C_{10}	21.9	(38.9–39.0)	(43.4)	47.7–48.4	53.9
C_5	C_{12}	29.6	50.9	—	55.3–55.5	56.5–56.6
C_6	C_7	13.6 ³	—	—	35.8–36.5	50.3
C_6	C_8	24.8	—	—	45.4–45.9	46.9
C_6	C_9	11.6	(38.3–38.7)	38.7–39.1	40.6–40.8	52.6–52.8
C_6	C_{10}	33.9	(45.0–45.2)	(46.3–46.4)	48.6–49.4	51.1
C_7	C_7	22.2	—	—	39.0–39.4	56.0–56.1
C_7	C_8	21.0	(26.1–26.2)	—	41.2–43.2	52.8–52.9
C_7	C_9	7.8	(43.3–43.4)	45.0–45.5 ⁴	45.5	58.0–58.1
C_7	C_{10}	16.8	(41.1–41.5)	49.5–49.7	51.1–51.2	55.8–55.9
C_7	C_{12}	31.2	53.1–53.3	—	—	60.5–60.8
C_8	C_7	22.6 ⁵	—	—	32.2–33.7	53.3
		23.5	—	—	38.7–39.4	—
C_8	C_9	21.6	37.9–38.8	48.3–48.6	49.3	56.4–56.5
C_8	C_{10}	31.8	50.9–51.5	—	53.6–53.8	54.8–55.0
C_{10}	C_9	20.7	46.3–47.0	—	56.2–56.3	58.3–58.4
C_{10}	C_{10}	35.9	52.0–52.3	—	—	59.4–59.6
C_{10}	C_{12}	45.0	64.2–64.6	—	—	67.4–67.5

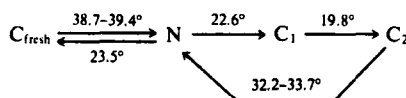
¹ C = crystallization temperature at a cooling rate of 2°/min.

² () indicates a monotropic transition.

³ A crystal-to-crystal transition occurs at 32.4–35°.

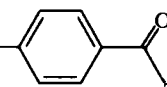
⁴ This is actually a $C \rightarrow S_{AN}$ transition.

⁵ Several crystal forms and two melting points were observed:



types of mesophases observed than the effect of changing the length of the alkoxy group on the acid portion. In this series, all the homologs studied exhibited a nematic, smectic A and smectic C combination with a monotropic biaxial smectic B type phase occurring below the smectic C phase. Again the smectic Y phase occurs at a shorter alkyl chain length and a smectic B plus smectic X combination or only a smectic B phase at longer chain lengths. We have also observed this difference in the effect of the two terminal chains on the types of mesophases observed in the oxy-esters.⁵ We feel it is due to the fact

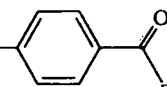
TABLE III

T_{CM} (°C) values for X--C₃

<i>X</i>	<i>Z</i>	
	O ^a	<i>S</i>
C ₇ O	42	36.9
C ₈ O	56	58.6
C ₉ O	61	62.6
C ₁₀ O	55	60.9

^aData from Ref. 14.

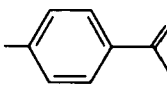
TABLE IV

T_{NI} (°C) values for X--C₃

<i>X</i>	<i>Z</i>	
	O ^a	<i>S</i>
C ₇ O	61	82.9
C ₈ O	66	86.9
C ₉ O	66	84.6
C ₁₀ O	69	85.6

^aData from Ref. 14.

TABLE V

Types of mesophases for X--C₃

<i>Z</i> = O ^a	<i>X</i>	<i>Z</i> = <i>S</i> phases
<i>X</i> = C ₇ -C ₁₀ O <i>S_A</i> + <i>N</i>	C ₇ O	(<i>S_C</i>) + <i>N</i>
	C ₈ -C ₁₁ O	(<i>S_T</i>) ^b + (<i>S_C</i>) + <i>S_A</i> + <i>N</i>
	C ₁₂ O	(<i>S_X</i>) + (<i>S_B</i>) + (<i>S_C</i>) + <i>S_A</i>
	C ₁₄ O	(<i>S_X</i>) + (<i>S_B</i>) + <i>S_A</i>
<i>X</i> = C ₇ <i>N</i>	C ₉ , C ₁₀	(<i>S_B</i>) + (<i>S_A</i>) + <i>N</i>
	C ₁₂	<i>S_B</i> + <i>N</i>

^aData from Ref. 14.

^b() indicates monotropic phase.

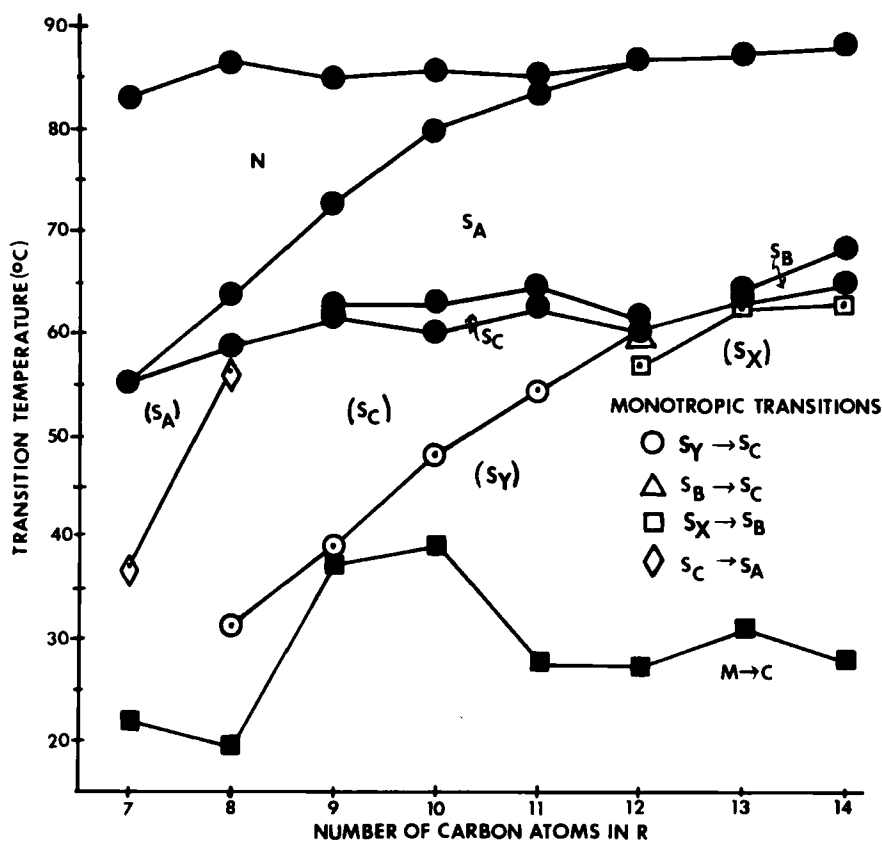


FIGURE 1 Transition temperatures versus the number of carbon atoms in the alkoxy chain for

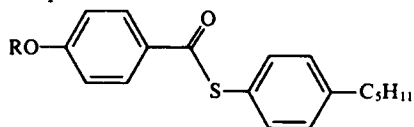


TABLE VI
Comparison of structures

Property	O	S	Effect on lateral forces
C—Z—C ^a angle	110°	104°	decreases
C—Z ^a bond	1.43 Å	1.81 Å	increases
Dipole Moment ^b (C ₆ H ₅) ₂ Z	0.99–1.36D	1.46–1.69	increases
Electronegativity ^c IR C=O	3.5 1724 cm	2.4 1670 cm	increases

^aData from Ref. 15.

^bData from Ref. 16.

^cData from Ref. 17.

^dData from Ref. 5.

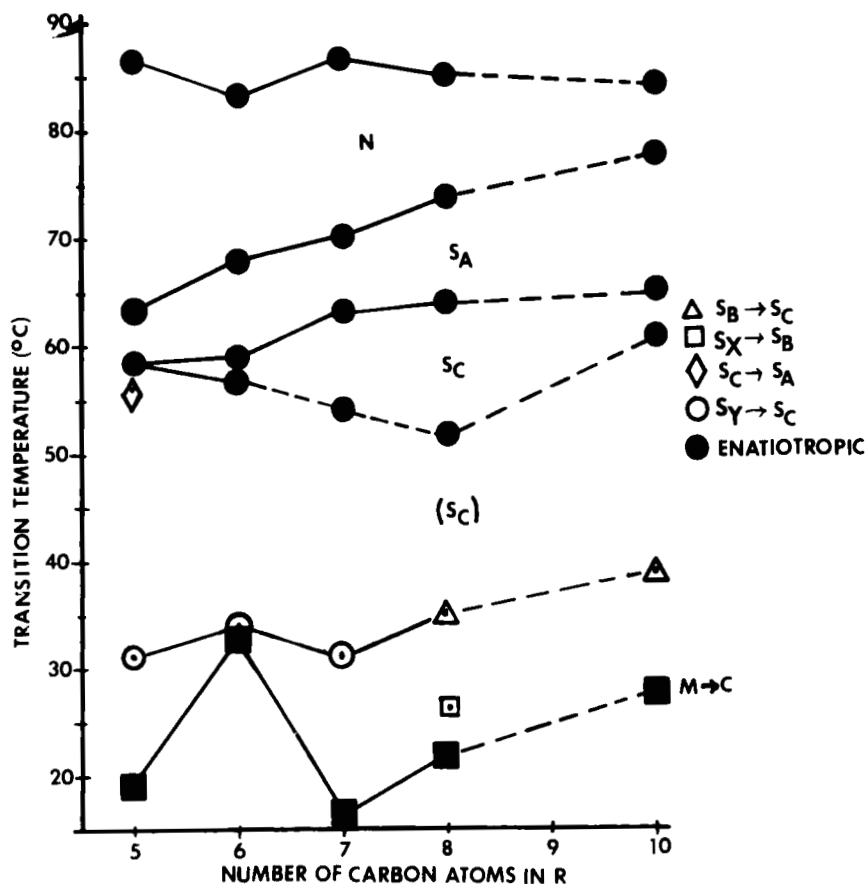
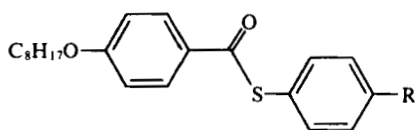
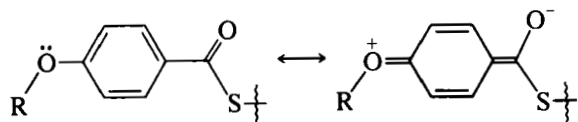


FIGURE 2 Transition temperature versus the number of carbon atoms in the alkyl chain for



that the alkoxy group can contribute to the resonance stability of the ring system in this manner:



This would influence the lateral forces between the molecules making the system more sensitive to changes in the alkoxy than in the alkyl group.

The effect of both substituents on the types of mesophases observed can be seen in a block diagram (Figure 3) of the type used by Goodby and Gray.²⁰ Since all the thioesters needed to fill in such a block diagram were not prepared in this work, we cannot be sure of the exact boundaries in some areas but we can see the approximate trends. When the alkoxy group (R) has a C_7 chain length, only a nematic plus smectic C combination was observed. But as soon as the chain length was increased by one carbon atom, a combination of nematic plus at least three smectic phases was found. Increasing the alkoxy chain length beyond C_{10} or C_{11} leads to loss of the nematic phase to give compounds showing various combinations of smectic phases. A combination of smectics A , C and Y occurred at shorter alkyl chain length (R') whereas a combination of smectics A , C , B and X occurred at longer chain length. When $R > C_{11}$ and $R' = C_5$, the smectics B plus X combination replaces smectic Y . When both the alkyl and alkoxy chains become long, the smectic B phase drops out leaving a smectics A , C , X or smectics C , X combination.

Interestingly, the smectic C phase occurs in all these compounds except in $13S5$ and $14S5$ i.e. a long alkoxy chain with a short alkyl group. Smectic A phases were always observed except when R is too short ($7SR'$) or both groups are too long ($14S10$).

MICROSCOPIC STUDIES

Microscopic textures for the dialkyl thioesters (1 , $X = R$, $Y = R'$) which showed only nematic, smectic A and smectic B phases were those which are typically observed for these phases (see for example Refs. 4 and 21). A uniaxial cross was observed in homeotropic textures for the smectics A and B phases. Transition bars were observed between the smectic A and B fan textures supporting the smectic B phase identification. The smectic B phase showed only a mosaic texture when it occurred below a nematic phase or by itself. Figure 4 shows the mosaic texture observed in the smectic B phase of $10S8$.

The microscopic textures shown in Figures 5a–5d for $8S5$ serve as typical examples of the textures observed in the smectics A , C , Y sequence. Figure 5a shows the typical smectic A fan texture which on cooling changes to the smectic C fan texture (Figure 5b) which continues to change on cooling to give the texture shown in Figure 5c. This indicates that the smectic C phase has a temperature dependent tilt angle. This was confirmed by X-ray diffraction studies.¹⁸ Further cooling gave the mosaic texture of the smectic Y phase (5d). We were unable to ever obtain a fan texture for this phase. Further cooling gave the crystalline phase. Conoscopic studies showed the disappearance of the uniaxial cross observed in the homeotropic texture of the smectic A phase on cooling into the schlieren texture of the smectic C phase. The center of the non-centered biaxial cross observed in this phase (Figure 6a) moved gradually out of the field of view (Figures 6b and 6c) on cooling into the smectic Y phase.

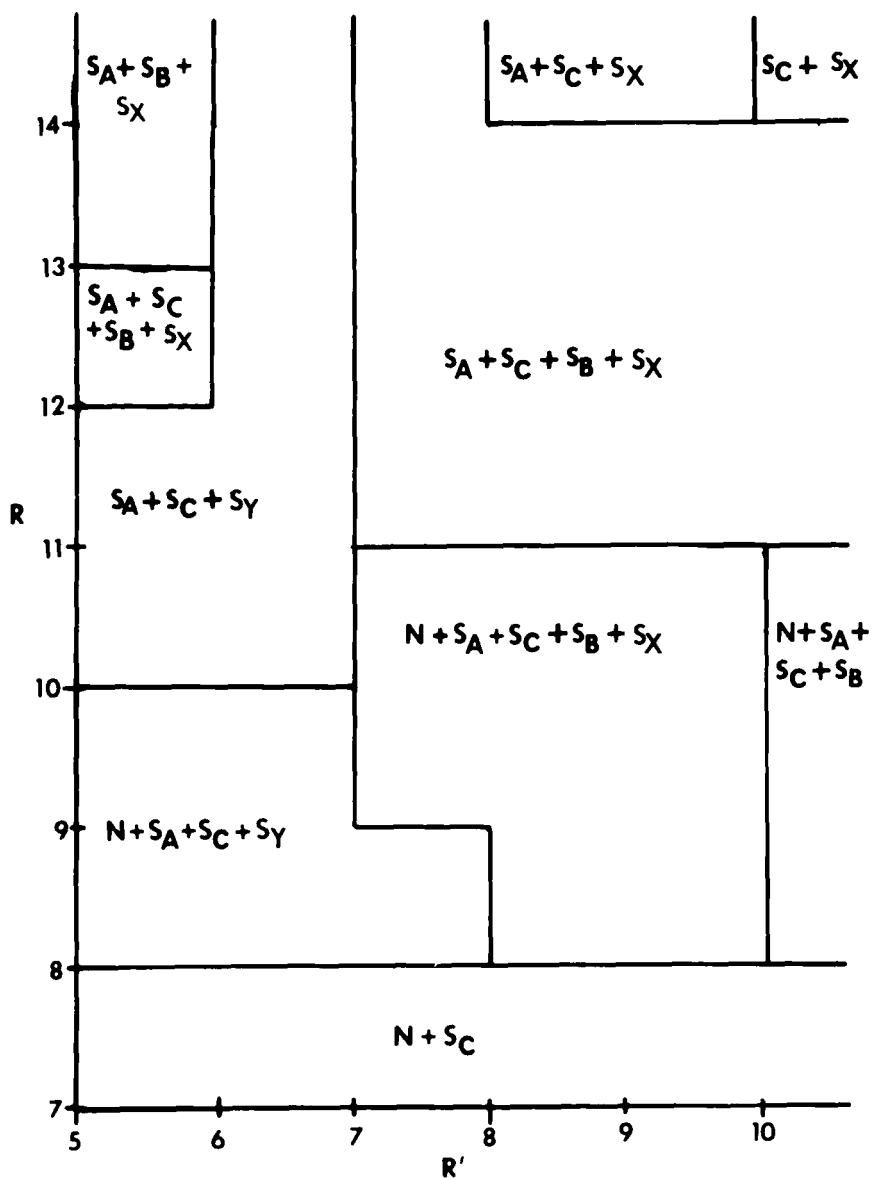
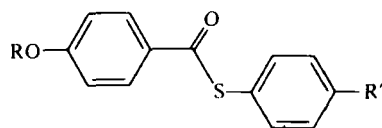


FIGURE 3 A block diagram plot of the types of mesophases observed in



when both the alkoxy and alkyl groups are varied.

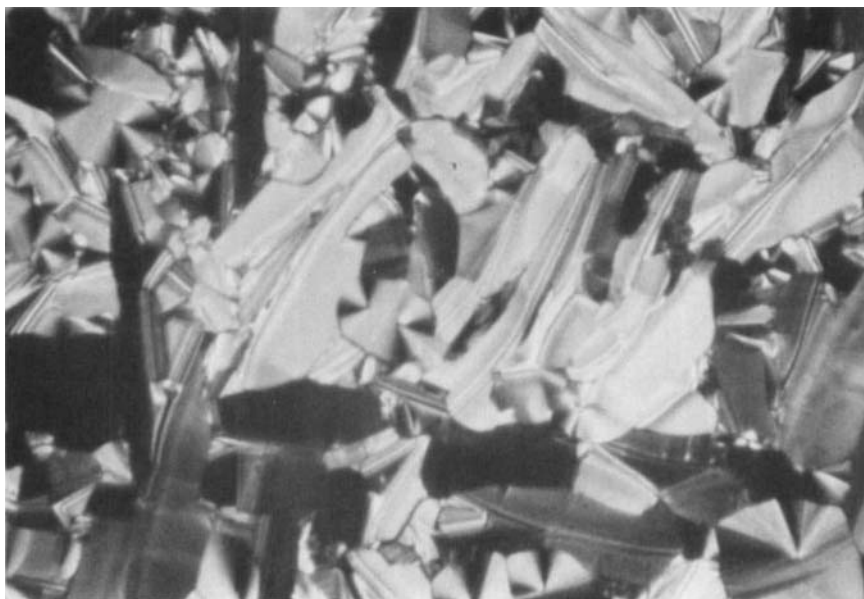


FIGURE 4 Mosaic texture for the smectic *B* phase in 10S8, $T = 52.4^{\circ}\text{C}$, $M = 16 \times 6$.

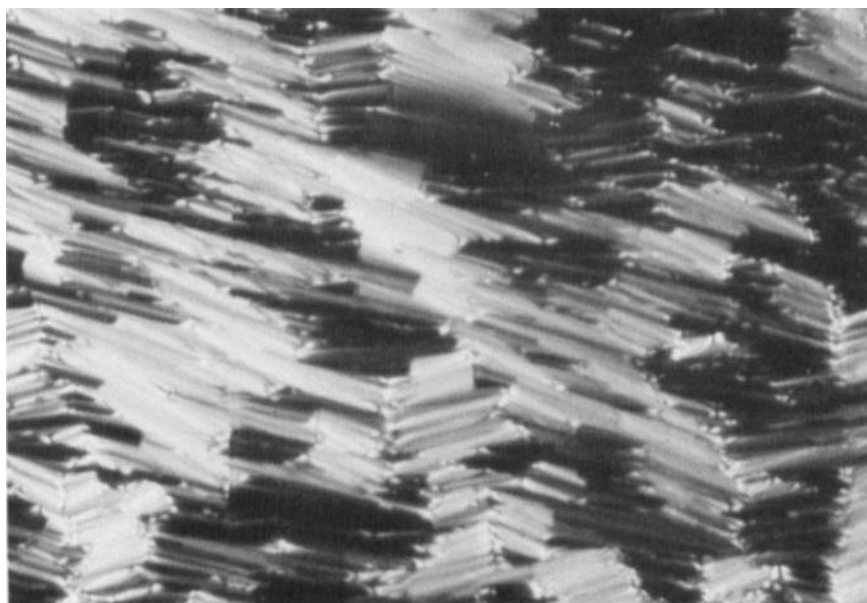
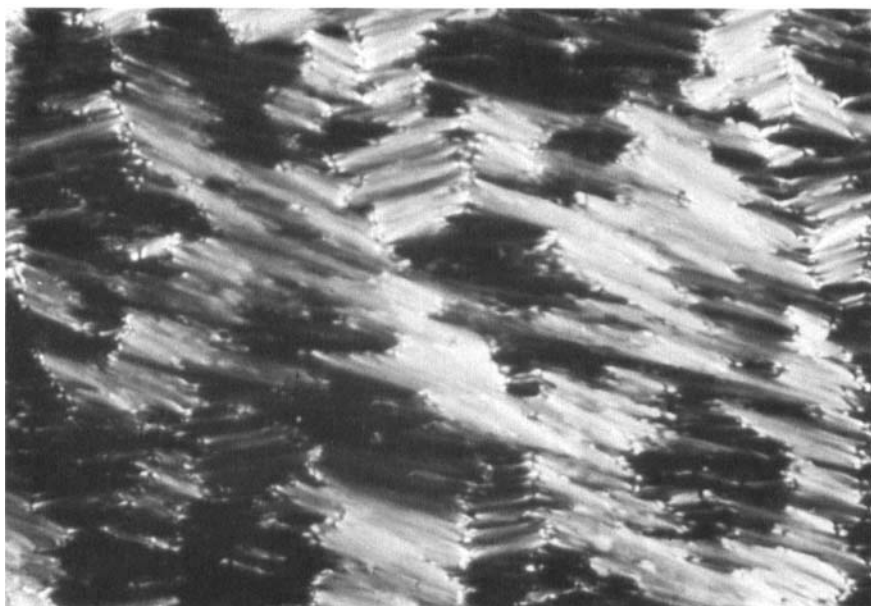
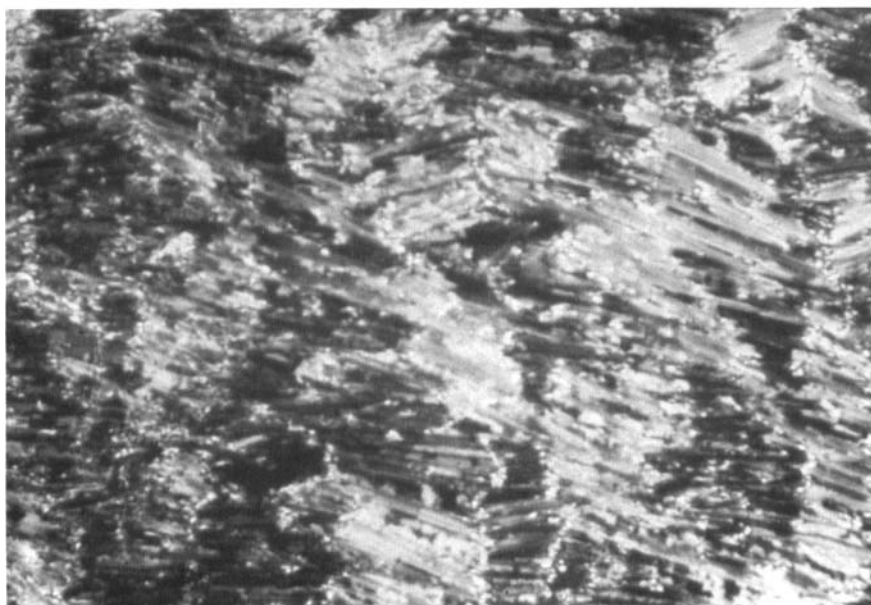


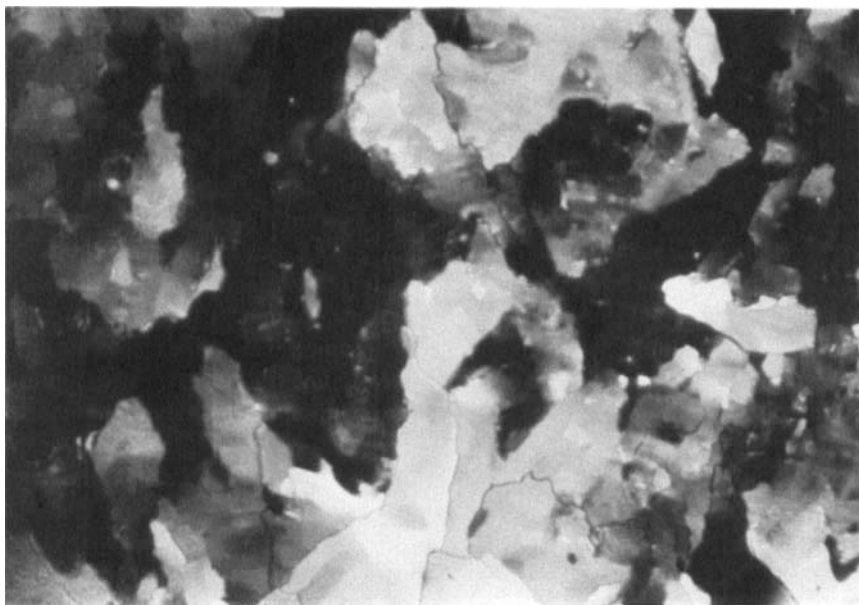
FIGURE 5 Fan textures for the smectic phases in $\bar{8}S5$, $M = 16 \times 6$. a. smectic *A* phase, $T = 61.5^{\circ}\text{C}$. b. smectic *C* phase, $T = 54.5^{\circ}\text{C}$. c. smectic *C* phase, $T = 33.4^{\circ}\text{C}$. d. smectic *Y* phase, $T = 29.2^{\circ}\text{C}$.



(5b)



(5c)



(5d)

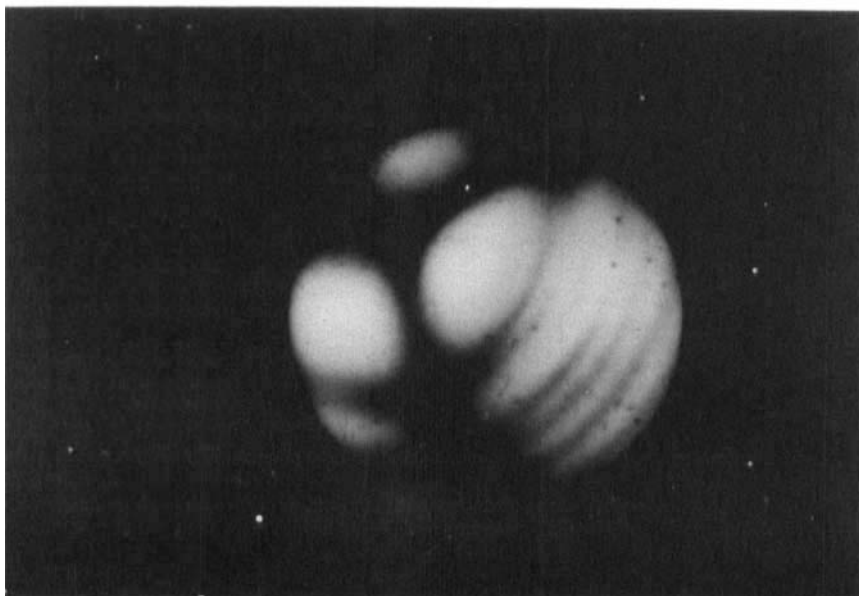
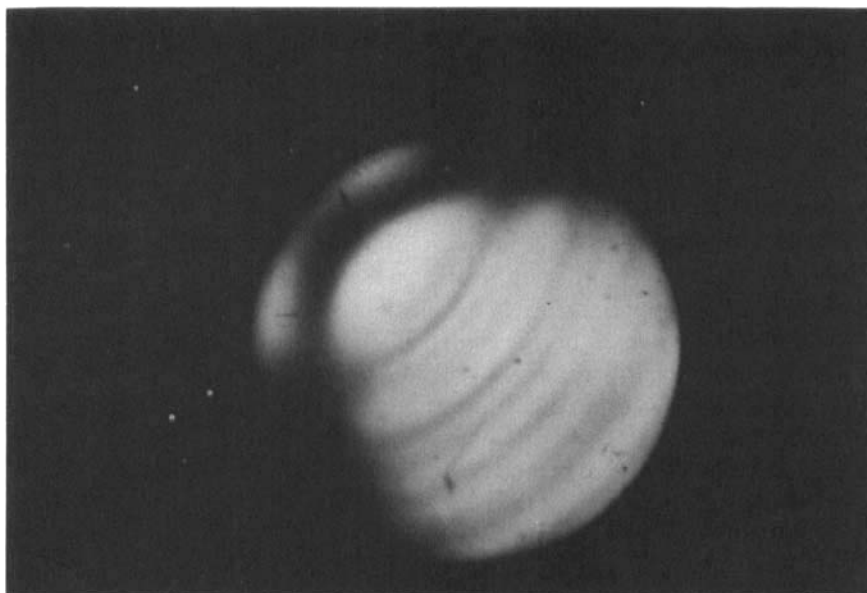
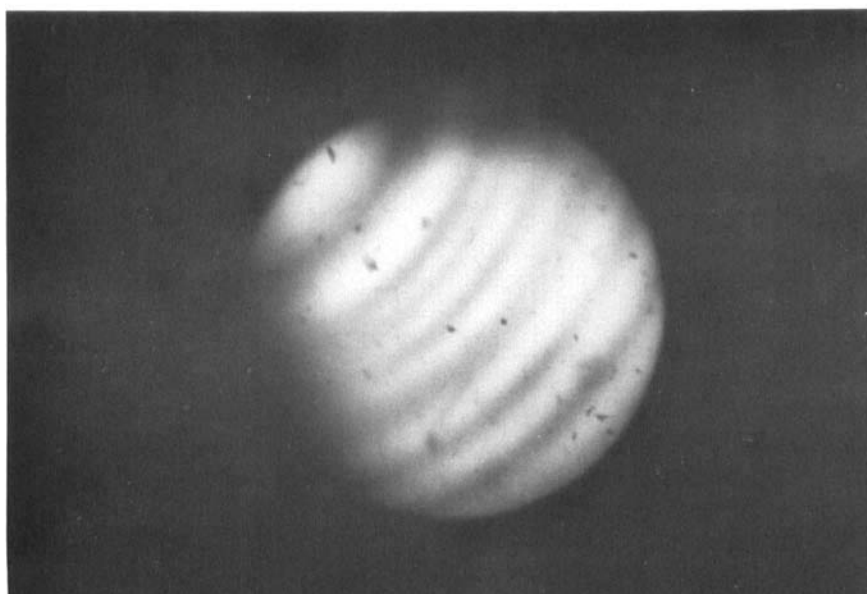


FIGURE 6 Conoscopic studies for $\bar{8}S5$, $M = 10 \times 50$. a. biaxial cross for smectic *C* phase, $T = 51.4^\circ\text{C}$. b. biaxial cross for smectic *C* phase, $T = 48.0^\circ\text{C}$. c. biaxial cross for smectic *C* phase, $T = 35.0^\circ\text{C}$. d. biaxial cross for smectic *Y* phase, $T = 27.5^\circ\text{C}$ (not the same sample as used in 6c).



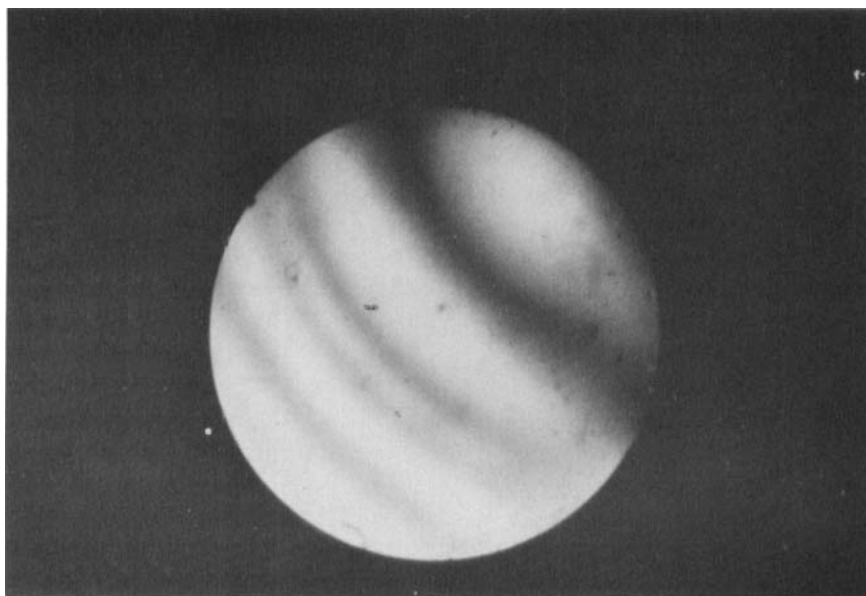
(6b)



(6c)

Only the colored rings of one isogyre of the biaxial cross could be seen (Figure 6d).

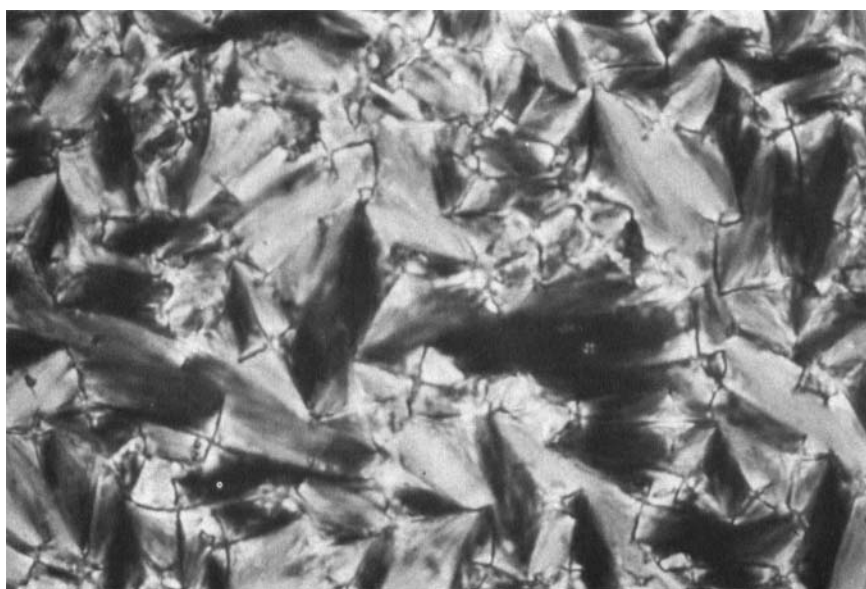
Those compounds which exhibited a smectic *B* plus smectic *X* transition such as $\overline{12S5}$ showed subtle continuous changes in the smectic *B* fan texture (Figure 7a) as it was cooled to the smectic *X* phase (Figure 7b). This change was gradual and can be seen better in a homeotropic area. Under normal lighting conditions, this area at first appears to be black, as in the smectic *B* phase, but with some texture. It is more apparent in the over-exposed (but equally exposed) photographs shown in Figures 8a–8c for $\overline{14S5}$. Figure 8a shows the smectic *B* phase with no texture in the black homeotropic region. On cooling into the smectic *X* phase, this area assumes some texture as seen in Figure 8b. This continues to change gradually on cooling until the texture becomes quite obvious in Figure 8c as that of a gray mosaic. In conoscopic studies, the uniaxial cross observed in the smectic *B* phase (Figure 9a) gradually becomes fainter as it converts to a centered biaxial cross (Figures 9b and 9c). The isogyres also move away from the center of the cross as the sample is cooled (Figure 9d). A hysteresis effect occurs; the isogyres are separated after cooling approximately 4.5° from the beginning of the transition whereas on reheating this difference is much smaller. More detailed optical studies are reported in Ref. 18a. These observations are very similar to those observed for a potassium palmitate lyotropic system.²² In several of these compounds, this transition occurs near the crystallization temperature making it difficult to study.



(6d)



FIGURE 7 Fan textures for smectic phases in $\overline{12}S5$, $M = 10 \times 32$. a. smectic B fan texture, $T = 59.2^\circ\text{C}$. b. smectic X fan texture, $T = 55.0^\circ\text{C}$.



(7b)

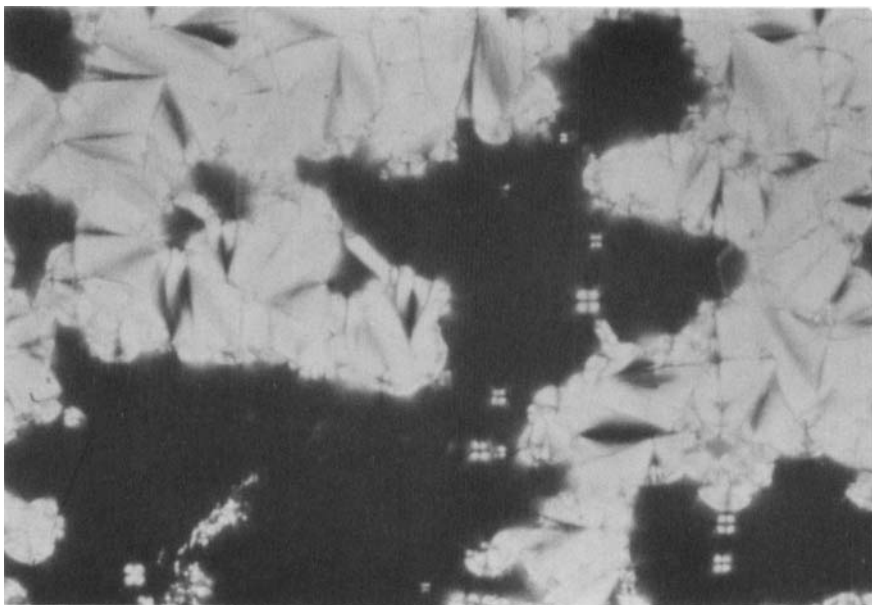
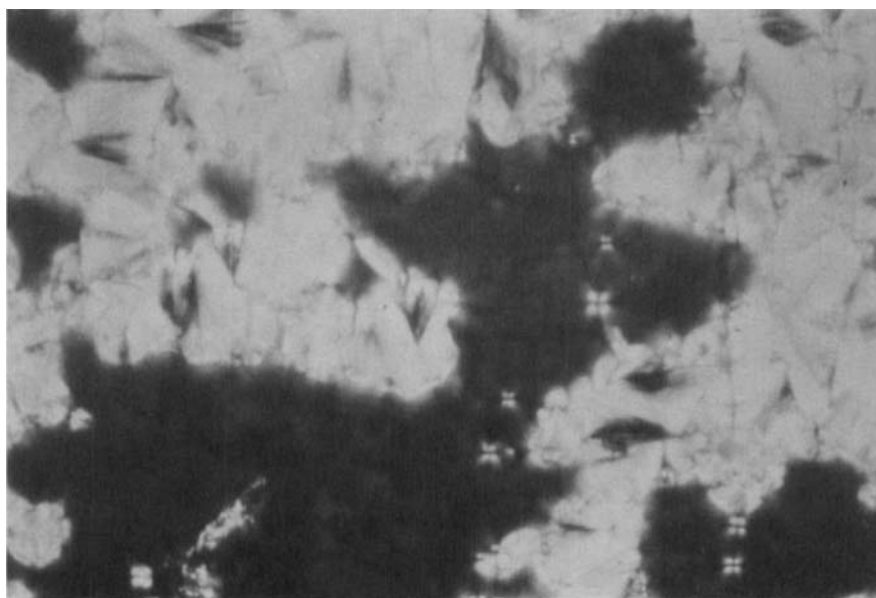
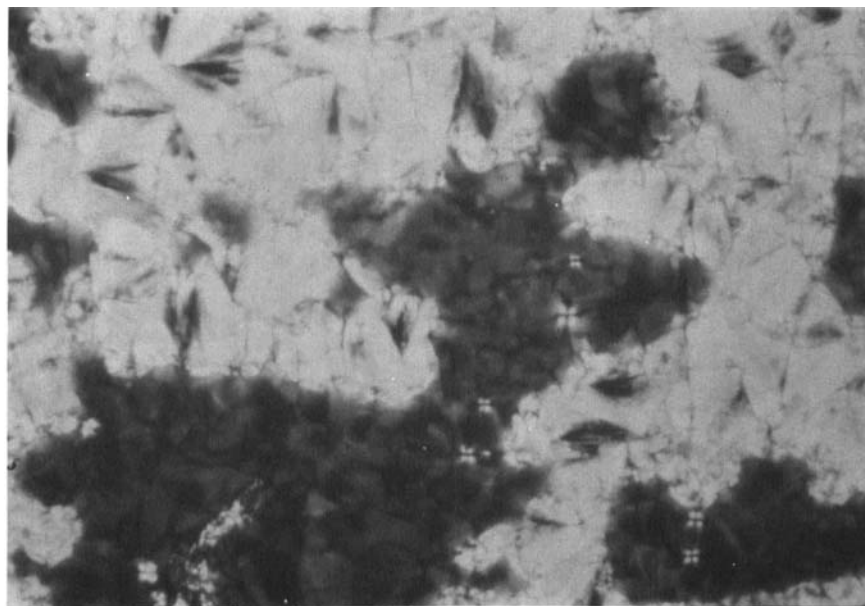


FIGURE 8 Homeotropic plus fan texture areas for the smectic phases in $\overline{14S5}$, $M = 10 \times 32$. a. smectic B phase, $T = 67.5^\circ\text{C}$. b. smectic X phase, $T = 60.4^\circ\text{C}$. c. smectic X phase, $T = 55.0^\circ\text{C}$.



(8b)



(8c)

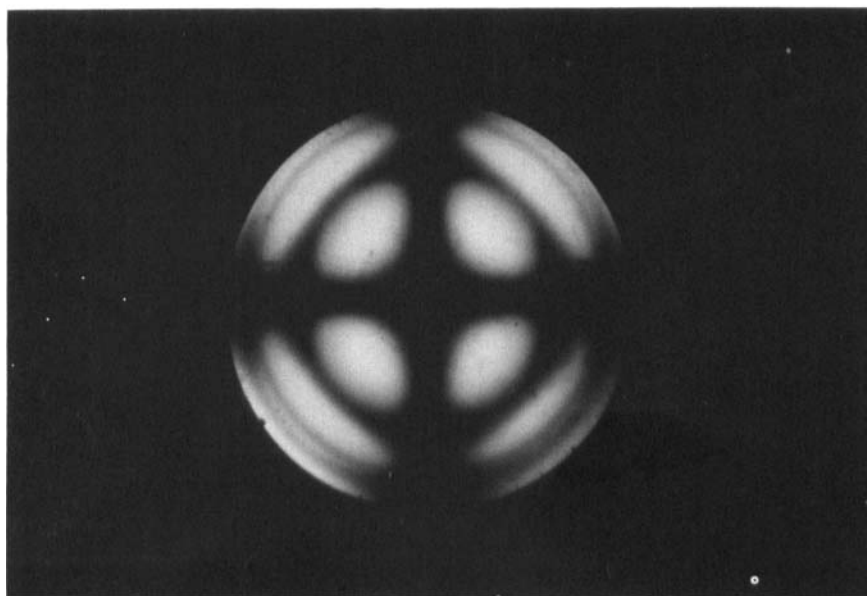
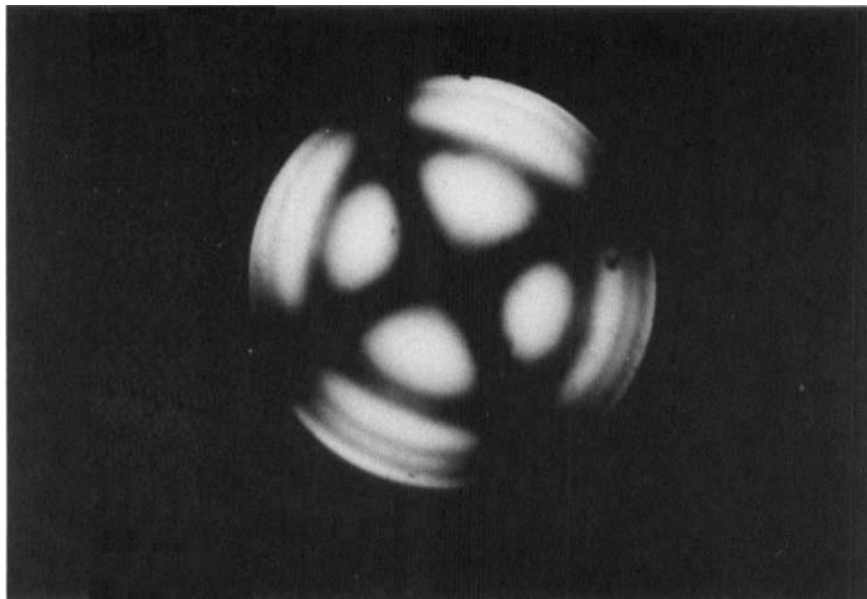
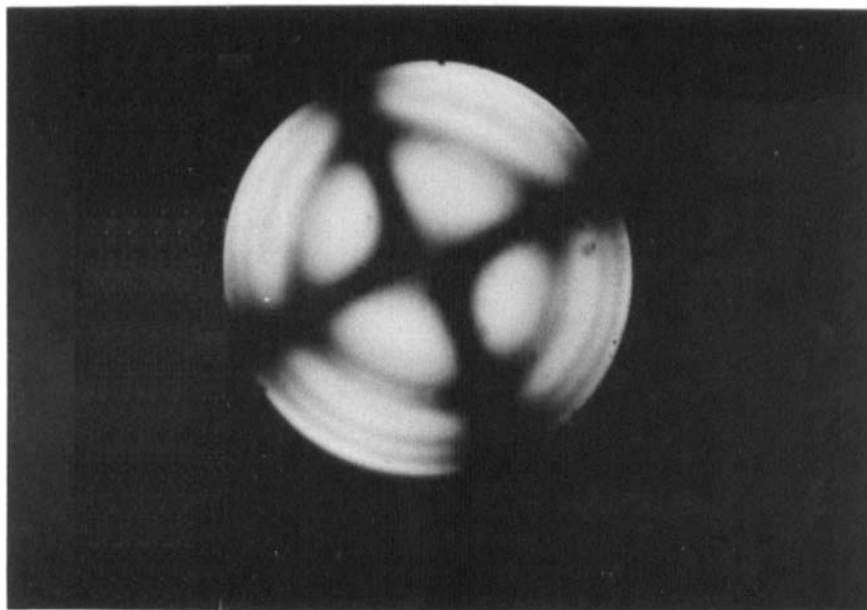


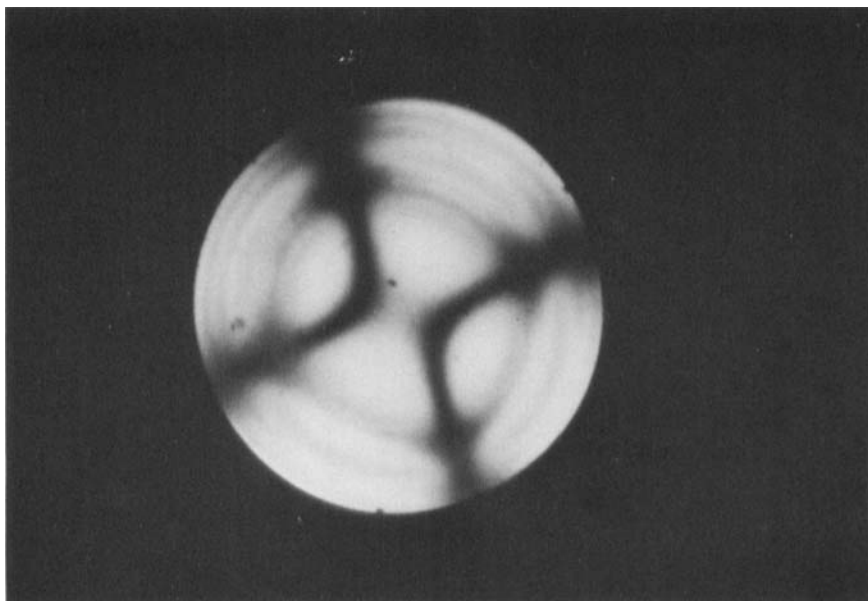
FIGURE 9 Conoscopic studies for $\overline{14S5}$, $M = 10 \times 50$. a. smectic B phase, $T = 62.4^\circ\text{C}$. b. smectic X phase, $T = 62.0^\circ\text{C}$. c. smectic X phase, $T = 61.7^\circ\text{C}$. d. smectic X phase, $T = 60.0^\circ\text{C}$.



(9b)



(9c)



(9d)

In $\overline{14S8}$ and $\overline{14S10}$, the smectic *B* phase disappears leaving only a biaxial phase. This showed a broken fan texture (Figure 10) and powder X-ray diffraction studies showed a smectic *B* type structure.¹⁸ However, we were unable to obtain a good single domain in conoscopic studies in order to determine whether this phase has a centered or non-centered biaxial cross and therefore whether it is a smectic *Y* or a smectic *X* phase. Its position in the homologous series would suggest this is a smectic *X* phase.

Fan textures for the smectic *A* phases observed in these compounds were obtained when both the slide and the cover slip were rubbed in the same direction parallel to the slide. When the slide was rubbed but not the cover slip, the domain textures (Figure 11) were observed at the nematic-to-smectic *A* transition for $\overline{8S5}$. The domain regions became smaller on cooling as shown in Figures 11a–11c.

DSC DATA

Thermal parameters (ΔH and ΔS) obtained by differential scanning calorimetry (DSC) for the $\overline{RS5}$ series are given in Table VII. Smectic *A*–*C* transitions did not show large enough peaks to be measurable. A plot of ΔH values versus alkoxy chain length for the melting transitions (Figure 12) shows a general rising trend despite the increasing order of the mesophases involved in this

TABLE VII

<i>R</i>	<i>T</i> (°C)	Transition type	ΔH^* (kcal/mole)	ΔS (cal/mole)
<i>C</i> ₇	55.02	<i>C</i> to <i>N</i>	6.450	19.6
	83.74	<i>N</i> to <i>I</i>	0.244	0.684
	(35.85)	<i>S</i> _A to <i>S</i> _C	0.099	0.320
	(23.35)	<i>S</i> _C to <i>C</i>	5.03	17.0
<i>C</i> ₈	59.06	<i>C</i> to <i>S</i> _A	7.910	23.8
	63.12	<i>S</i> _A to <i>N</i>	0.035	0.104
	86.88	<i>N</i> to <i>I</i>	0.333	0.925
	(28.85)	<i>S</i> _A to <i>S</i> _Y	0.713	2.36
	(18.92)	<i>S</i> _Y to <i>C</i>	5.01	17.2
<i>C</i> ₉	63.48	<i>C</i> to <i>S</i> _{CA}	8.520	25.3
	74.20	<i>S</i> _A to <i>N</i>	0.092	0.265
	85.99	<i>N</i> to <i>I</i>	0.350	0.975
	(40.15)	<i>S</i> _C to <i>S</i> _Y	0.688	2.20
	(39.35)	<i>S</i> _Y to <i>C</i>	1.670	5.34
<i>C</i> ₁₀	65.68	<i>C</i> to <i>S</i> _{CA}	9.260	27.3
	81.14	<i>S</i> _A to <i>N</i>	0.233	0.658
	87.06	<i>N</i> to <i>I</i>	0.448	1.24
	(48.22)	<i>S</i> _C to <i>S</i> _Y	0.803	2.50
	(40.66)	<i>S</i> _Y to <i>C</i>	1.630	5.19
<i>C</i> ₁₁	64.92	<i>C</i> ₁ to <i>S</i> _C	9.11	26.9
	63.67	<i>C</i> ₂ to <i>S</i> _C	8.68	25.7
	85.09	<i>S</i> _A to <i>N</i>	0.466	1.30
	86.75	<i>N</i> to <i>I</i>	0.490	1.36
	(55.48)	<i>S</i> _C to <i>S</i> _X	0.865	2.63
	27.35	<i>S</i> _X to <i>C</i>	4.16	13.8
<i>C</i> ₁₂	62.10	<i>C</i> to <i>S</i> _{CA}	8.150	24.3
	86.97	<i>S</i> _A to <i>I</i>	1.660	4.61
	(59.6)	<i>S</i> _C to <i>S</i> _B	0.943	2.83
	(56.1)	<i>S</i> _B to <i>S</i> _Y	0.015	0.046
	(21.6)	<i>S</i> _Y to <i>C</i>	2.59	8.79
<i>C</i> ₁₃	66.04	<i>C</i> ₁ to <i>S</i> _B	9.00	26.3
	63.84	<i>C</i> ₂ to <i>S</i> _B	7.92	23.5
	65.24	<i>S</i> _B to <i>S</i> _A	1.08	3.18
	88.66	<i>S</i> _A to <i>I</i>	1.86	5.14
	(62.62)	<i>S</i> _B to <i>S</i> _Y	0.013	0.0039
<i>C</i> ₁₄	30.79	<i>S</i> _Y to <i>C</i>	6.40	21.1
	68.84	<i>C</i> to <i>S</i> _{BA}	10.760	31.50
	88.5	<i>S</i> _A to <i>I</i>	1.870	5.17
	68.22	<i>S</i> _A to <i>S</i> _B	1.250	3.66
	(61.76)	<i>S</i> _B to <i>S</i> _Y	0.0005	0.0015
	(29)	<i>S</i> _Y to <i>C</i>	5.460	8.10

* Standard deviation = 0.004–0.500 for 3–6 runs.

transition. From this, it appears that the effect of increasing alkoxy chain length on the ΔH values is greater than the effect of increasing order of the mesophases involved. A plot of ΔS values shows the same trends.

It is interesting to see a sharp fall to a minimum at $R = C_{12}$ in this curve. Since the C_{11} and C_{12} homologs both involve a crystal to smectic *C* transition, this minimum cannot be explained by a transition to a different type of meso-

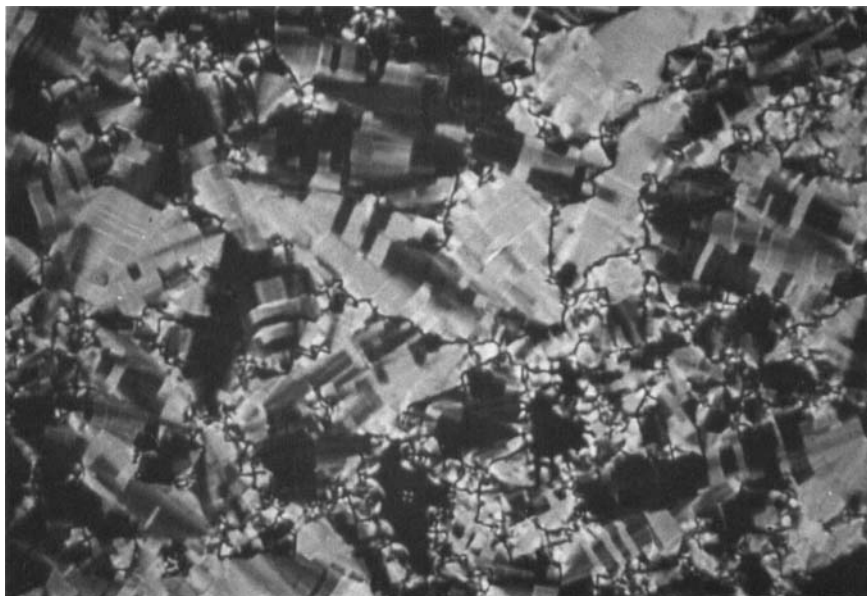


FIGURE 10 Fan texture for smectic *B* phase in $\overline{14S10}$, $T = 80.6^\circ$, $M = 10 \times 32$.

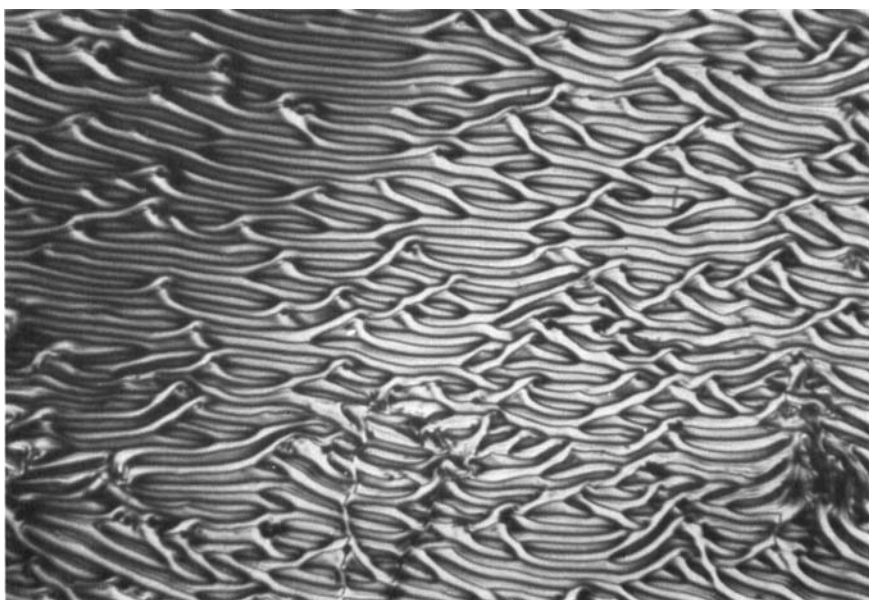
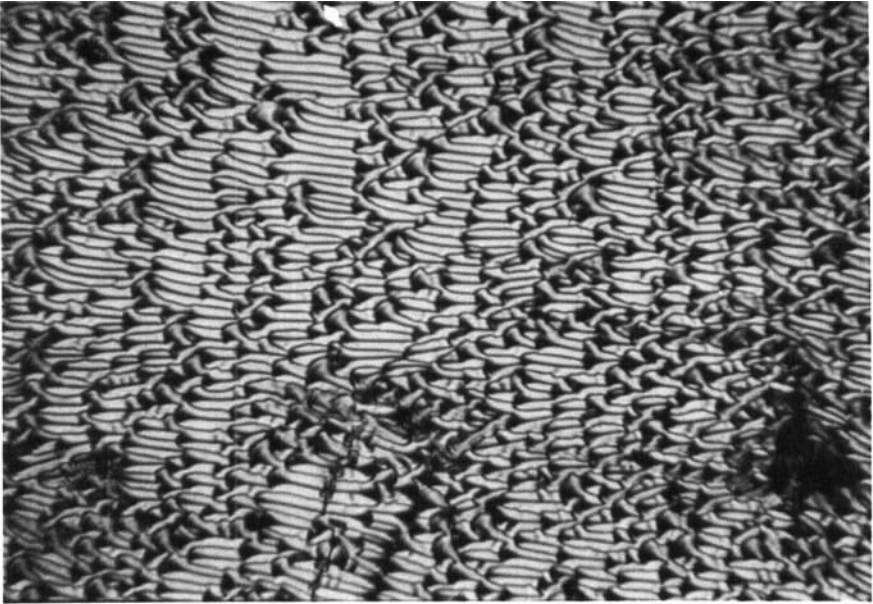
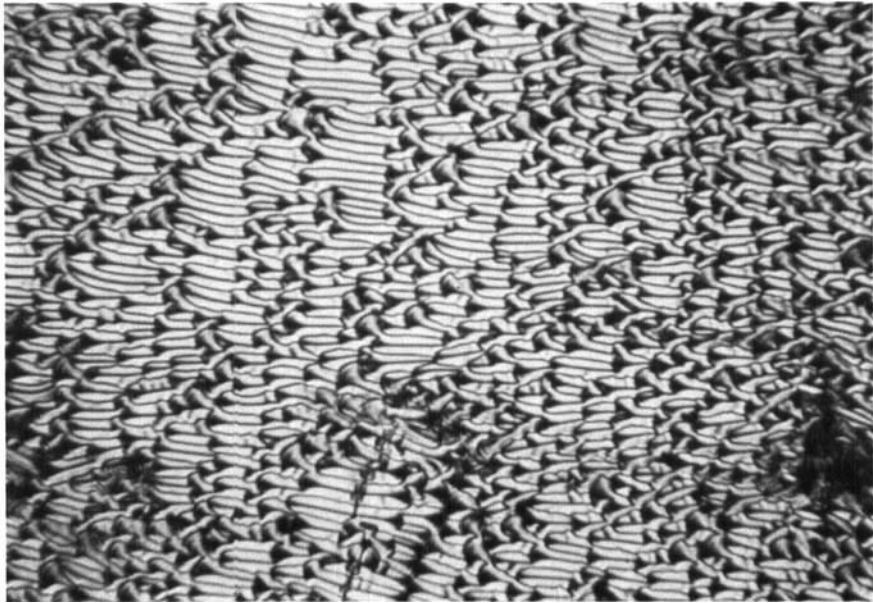


FIGURE 11 Texture obtained for the smectic *A* phase in $\overline{8S5}$ with plates having different alignments, $M = 6 \times 16$. a. $T = 63.0^\circ\text{C}$. b. $T = 62.9^\circ\text{C}$. c. $T = 62.8^\circ\text{C}$.



(11b)



(11c)

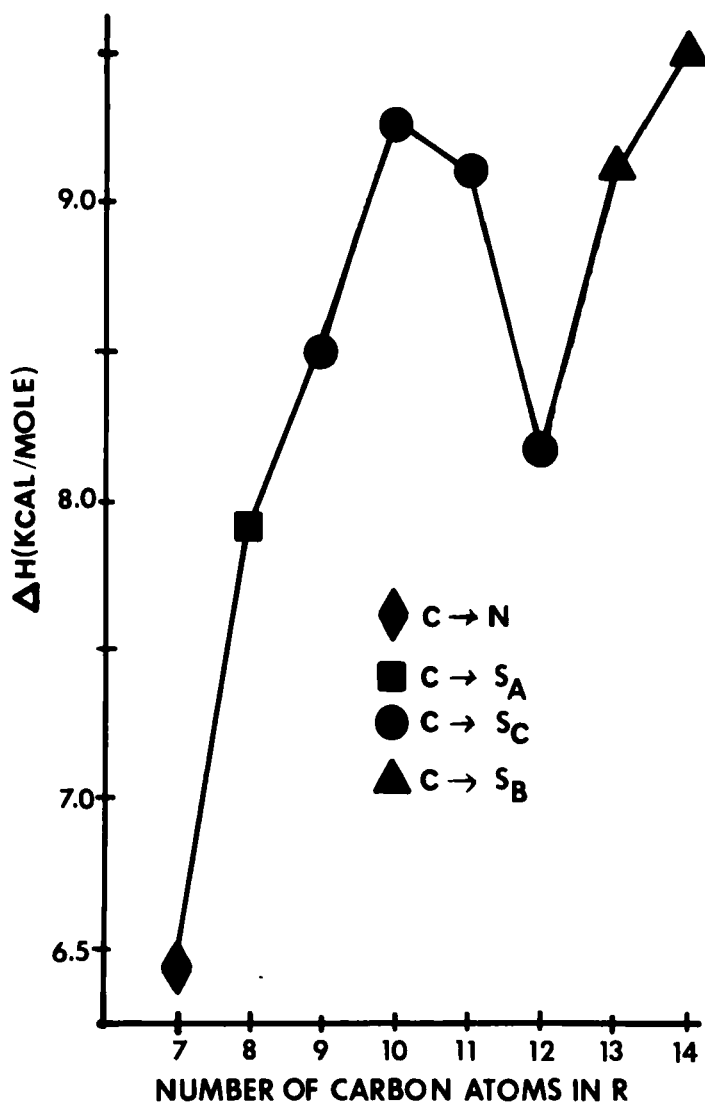
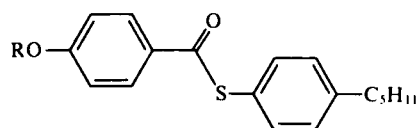


FIGURE 12 ΔH for melting transitions versus the number of carbon atoms in the alkoxy group for



phase. However, we cannot be sure that the same type of crystal structure is involved in this transition for all these homologs. In DSC scans, both the C_{11} and C_{13} homologs showed crystal-to-crystal transitions but this was not true of the C_{12} homolog. It is quite possible that we have not observed all the crystalline states present in these compounds.

That the thermal history of the solid state of these thioesters is more complex than we have shown is supported by calorimetric data from Janik's laboratory and microscopy data from the Halle group.²³ Janik found several low temperature crystalline changes for $\bar{7}S5$; a comparison of our DSC data with his calorimetric data is given in Table VIII. The large difference in values for the nematic to isotropic transition is probably due to the large experimental error in the DSC data. The Halle group reports three different melting transitions as shown in Figure 13. Since we have been primarily interested in studying mesophases instead of the solid state, we have not spent sufficient time to unravel all the various crystal changes observed for these compounds. The crystal changes which we did observe in our DSC scans and in our routine collecting of transition temperatures are presented in Tables I, II and VII. Two melting temperatures were observed in $\bar{13}S5$ as well as a crystal-to-crystal change as shown in the DSC scan given in Figure 14.

A similar plot of ΔH values for the clearing transitions (Figure 15) shows a typical gradually rising trend for the nematic-to-isotropic transitions with in-

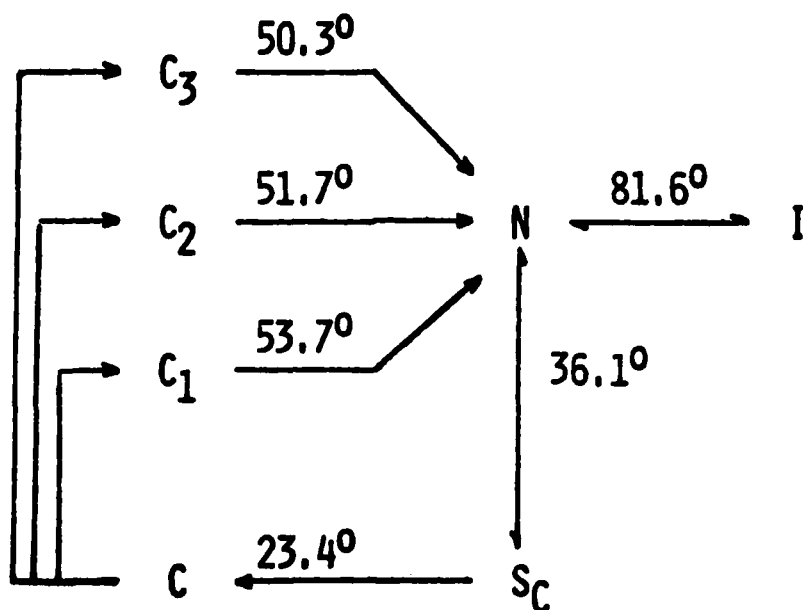


FIGURE 13 Microscopic transitions for $\bar{7}S5$ obtained by the Halle Group.

TABLE VIII
Calorimetry data for $\bar{7}S5$

Method	Temp (°C)	Phase transition	ΔH kcal/mole	ΔS cal/mole
DSC	55.02	C to N	6.45	19.6
	83.74	N to I	0.24	0.68
Calorimetry (Janik)	-89.62	C_3 to C_2	0.279	1.44
	-1.15	C_2 to C_1	0.054	0.21
	52.72	C_1 to N	6.18	21.10
	79.05	N to I	0.61	1.28

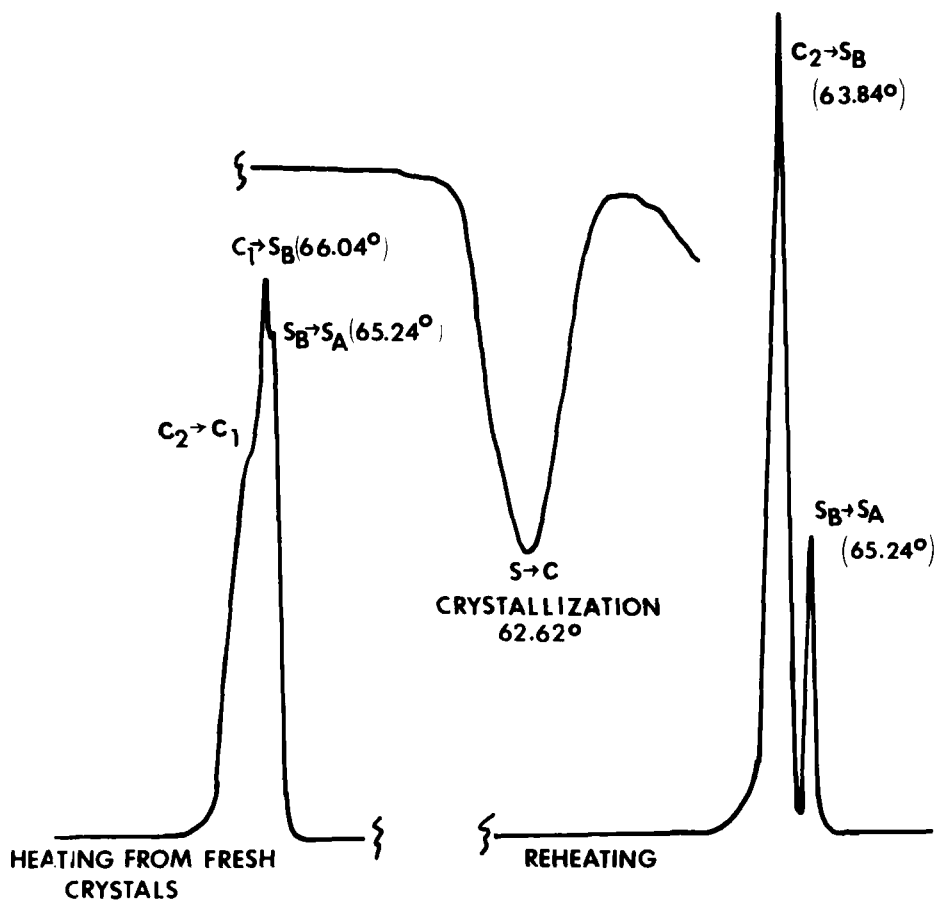


FIGURE 14 DSC scan for $C_{13}H_{27}O-C_6H_4-CO-S-C_6H_4-C_5H_{11}$

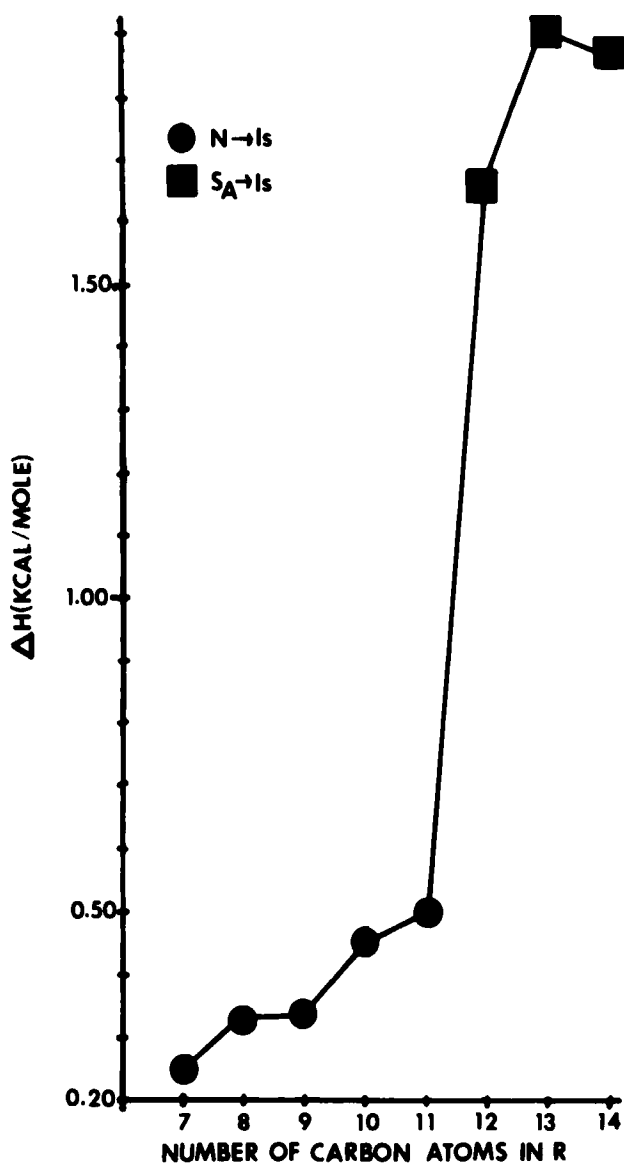
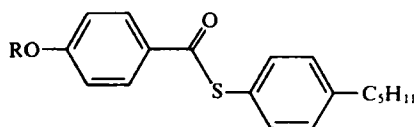


FIGURE 15 ΔH for mesophase to isotropic transitions versus the number of carbon atoms in the alkoxy group for



creasing alkoxy chain length followed by a sharp increase when the clearing transition becomes a smectic *A* to isotropic transition. This is what would be expected to occur from the effect of increasing chain length on the ΔH values.

A DSC scan for $\overline{12S5}$ (Figure 16) shows the small thermal heat change observed for the smectic *B*-*X* transition. This becomes even smaller for $\overline{14S5}$ (see Table VII) but unlike the smectic *A*-*C* transition, it is still measurable.

CONCLUSIONS

We have prepared a variety of alkoxy-alkyl and dialkyl thioesters **1** and compared their mesomorphic properties with those found for the oxy-esters. In general, melting temperatures were approximately the same in both series but

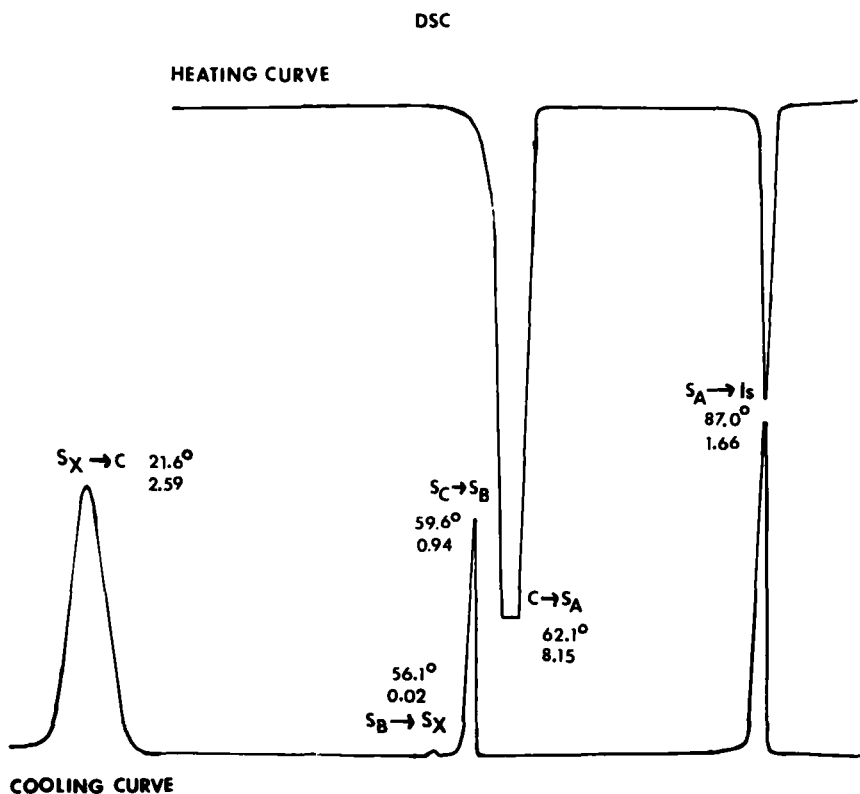


FIGURE 16 DSC scan for $C_{12}H_{25}O-C_6H_4-CO-S-C_6H_4-C_3H_{11}$

nematic-to-isotropic temperatures were higher. This structural change also seems to favor the formation of smectic phases as well as a greater variety of them.

Only nematic, smectic *C* and smectic *B* phases were observed in the dialkyl series but nematic, smectics *A*, *C* and *B* were found in the alkoxy-alkyl series along with two as yet unidentified smectic *B* type biaxial phases. One of these biaxial phases, S_y , occurs below a smectic *C* phase and was found to have a non-centered biaxial conoscopic cross with its center outside the field of view.

De Vries feels this is another example of the smectic *I* phase.¹⁸ The other biaxial phase, S_x , occurs below a uniaxial smectic *B* phase and showed a centered biaxial conoscopic cross; the transition between the smectic *B* and *X* phases is second order. Mixture studies with known phases have not yet been performed on these compounds. However, considering the difficulties that were encountered in identifying the tilted smectic *B* type phase below the smectic *C* phase in TBBA (now identified as the smectic *G* phase) using mixture studies,^{24,25} it would seem that the biaxial smectic *B* type phases in these thioesters would be equally difficult to identify by mixture studies.

Thermal parameters were determined for the alkoxy- C_5 alkyl series. On increasing the alkoxy chain length, a rising curve was observed for both the melting and mesophase-to-isotropic transitions. However, the sharp dip in the melting curve at $R = C_{12}$ showed the problems involved in using DSC data to compare thermal parameters. The importance of including the ΔH values for all the transitions involved in melting has been discussed by Barrall and Johnson.^{26,27} Since mesomorphic compounds tend to show a variety of solid-solid transitions, this makes it difficult to compare ΔH of melting values obtained from DSC data for these compounds.

The interest in these thioesters is shown by the wide variety of physical studies which have been made using these compounds: DSC of mixtures,² calorimetry,^{3,23,28} nematic bend-splay elasticity,²⁹ optical birefringence,³⁰ deuteron spin-lattice relaxation in the nematic phase,³¹ X-ray crystallography^{18a} and temperature-pressure studies.³²

EXPERIMENTAL

Materials

N,N'-Dicyclohexylcarbodiimide and 4-dimethylaminopyridine were obtained from Aldrich Chemical Company and used without purification. Organic extracts were dried over anhyd. Na_2SO_4 followed by Linde No. 4A molecular sieves. Anal-Tech silica gel GHLF 2.5×10 cm Uniplates® (250μ) and UV light as the detector were used for thin-layer chromatography.

Techniques

A Perkin-Elmer model 700 (ir) and Varian A-60 (nmr, TMS internal standard in CDCl_3) were used as analytical tools. The elemental analysis was performed by Spang Microanalytical Laboratories, Ann Arbor, Michigan.

Transition temperatures and textures were determined using a Leitz-Wetzler ortholux polarizing microscope equipped with a calibrated, modified Mettler FP-2 heating stage at a rate of $2^\circ/\text{min}$. Smectic phases were identified using both homogeneously and homeotropically aligned samples along with conoscopic studies. Fan textures were studied using the method described in Ref. 21. Unlike the dianils studied in Ref. 21, these compounds appeared to be stable to reheating cycles.

Homeotropic textures were obtained by moving the cover slip while the sample was in its highest uniaxial mesophase. For conoscopic studies, the slides were pretreated with the aligning agent, *N,N*-dimethyl-*N*-octadecyl-3-aminopropyltrimethoxysilyl chloride (DMOAP or Dow-Corning XZ-2-2300) using Kahn's method.³³ Thick sample layers had to be used to obtain good biaxial crosses.

The photographs of microscopic fan textures and conoscopic crosses were taken using the microscope's Leica 35mm camera. The same area was maintained within each sequence of photographs unless otherwise noted. Magnification (M) = eyepiece \times objective powers. DSC data was obtained using a Perkin-Elmer DSC-2 instrument interfaced to a minicomputer (Digital Equipment Corporation, model PDP-11V03). Integrations of peak areas (used to determine enthalpy values) for peaks observed in heating scans were obtained on the computer using programs derived from the Perkin-Elmer DSC-4 program (Perkin-Elmer, Norwalk, Connecticut, USA). Peak areas for monotropic transitions often had to be determined by cutting and weighing copies of the peaks. In some instances both methods were used with the results agreeing to within the experimental error of $\sim 10\%$.

The DSC instrument was calibrated using indium standards. Entropy values were calculated using the equation, $\Delta S = \Delta H/T$. Samples were weighed by difference on a Perkin-Elmer AM-2 autobalance.

Two to three scans were run on each sample and at least two samples of each compound were run at scanning rates of 2 and 1 mcal/sec. The enthalpy values presented here represent an average of these values.

4-*n*-Pentylbenzenethio-4'-*n*-decyloxybenzoate, 1b ($X = \text{C}_{10}\text{H}_{21}$, $Y = \text{C}_5\text{H}_{11}$). A soln of 1.6g (5.5 mmoles) of 4-*n*-decyloxybenzoyl chloride in 4 ml CH_2Cl_2 was added dropwise to a stirred soln of 1.0 g (5.5 mmoles) of 4-*n*-pentylbenzenethiol and 0.85 ml Et_3N in 4 ml CH_2Cl_2 . Stirring was continued for 30 min at R.T. The rxn mixture was extracted with H_2O (to remove $\text{Et}_3\text{N} \cdot \text{HCl}$) 5% aq

KOH soln, H₂O and then dried, filtered and concentrated to dryness (Rotovap) to give 2.4 g (quantitative yield) of the crude thioester. This material was recrystallized 3× from abs EtOH–EtOAc (4:1) to give 1.30 g (53.7%) of the purified thioester, **1b** ($X = C_{10}H_{21}$, $Y = C_5H_{11}$): transition data is in Table I and tlc (CHCl₃) showed one spot with $R_f = 0.74$ (R_f for thiol = 0.75).

Anal. Calcd. for C₂₈H₄₀SO₂: C, 76.31; H, 9.15; S, 7.28. Found: C, 76.27; H, 9.09; S, 7.21.

Comparable yields were obtained using 15–40 g of one of the starting materials.

4-*n*-Pentylbenzenethio-4'-*n*-tetradecyloxybenzoate, **1b** ($X = C_{14}H_{29}$, $Y = C_5H_{11}$). To a mixture of 1.9 g (5.5 mmoles) of 4-*n*-tetradecyloxybenzoic acid (see Ref. 10 for synthesis), 1.0 g (5.5 mmoles) 4-*n*-pentylbenzenethiol and 27.5 mg of 4-dimethylaminopyridine in 10 ml CH₂Cl₂ was added 1.1 g (5.5 mmoles) of *N,N'*-dicyclohexylcarbodiimide. The reaction mixture was stirred and refluxed 4 hr. The insoluble *N,N'*-dicyclohexylurea was removed by filtration from the cooled reaction mixture and washed thoroughly with CH₂Cl₂. The filtrate was extracted with 3*N*HCl, 5% aq KOH and H₂O. The organic layer was dried, filtered and concentrated to dryness (Rotovap) to give 2.50 g (90.6%) of the crude thioester. This material was recrystallized 3× from abs EtOH to give 1.59 g (57.6%) of the purified thioester, **1b** ($X = C_{10}H_{21}$, $Y = C_5H_{11}$): transition temperatures are given in Table I; tlc (CHCl₃) showed only one spot, it showed a 1670 cm⁻¹ (COS) absorption and nmr (CDCl₃) δ 8.00 (d, 2, *J* = 8 Hz, ArH *ortho* to RO), 7.30 (m, 4, ArH *ortho* to C=O and Ar'H *ortho* to S), 6.90 (d, 2, *J* = 8 Hz, Ar'H *ortho* to alkyl), 4.0 (t, 2, ArOCH₂), 2.65 (t, 2, Ar'CH₂) and 0.6–2.2 (m, 36, C₁₃H₂₇ + C₄H₉).

Acknowledgments

We are indebted to the National Science Foundation for partial financial support for this research under grant numbers DMR-76-13173 and DMR-78-26495. We appreciate the contributions of T. Flood and the Chemistry Department for providing nmr spectra; S. J. Laskos, Jr., R. F. Griffith and M. E. Stahl for helping to prepare some of the intermediates; A. de Vries for providing X-ray data, J. T. S. Andrews for help on the DSC instrument and E. P. Pluddemann of Dow-Corning for the sample of XZ-2-2300.

References

1. R. M. Reynolds, C. Maze and E. Oppenheim, *Mol. Cryst. Liq. Cryst.* **36**, 41 (1976).
2. D. Johnson, D. Allender, R. de Hoff, C. Maze, E. Oppenheim and R. Reynolds, *Phys. Rev.*, **B 16**, 470 (1977).
3. D. Brisbin, R. de Hoff, T. E. Lockhart and D. L. Johnson, *Phys. Rev. Lett.*, **43**, 1171 (1979).
4. M. E. Neubert, J. P. Ferrato and R. E. Carpenter, *Mol. Cryst. Liq. Cryst.*, **53**, 229 (1979).
5. M. E. Neubert, L. T. Carlino, D. L. Fishel and R. M. D'Sidocky, *Mol. Cryst. Liq. Cryst.*, **59**, 253 (1980).

6. Y. B. Kim and M. Seno, *Mol. Cryst. Liq. Cryst.*, **36**, 293 (1976).
7. J. Krause and L. Pohl, Abstract I-3, Sixth International Liquid Crystal Conference, Kent, Ohio, 1976.
8. K. Praefcke, J. Martens, U. Schulze, H. Simon and G. Heppke, *Chem. Zeitung*, **101**, 450 (1977).
9. M. E. Neubert, S. J. Laskos, Jr., L. J. Maurer, L. T. Carlino and J. P. Ferrato, *Mol. Cryst. Liq. Cryst.*, **44**, 197 (1978).
10. M. E. Neubert and D. L. Fishel, *Mol. Cryst. Liq. Cryst.*, **53**, 101 (1979).
11. M. E. Neubert, S. J. Laskos, Jr., R. F. Griffith, M. E. Stahl and L. J. Maurer, *Mol. Cryst. Liq. Cryst.*, **54**, 221 (1979).
12. B. Neises and W. Steglich, *Angew. Chem. Int. Ed. Engl.*, **17**, 522 (1978).
13. F. E. Ziegler and G. D. Berger, *Synth. Commun.*, **9**, 539 (1979).
14. D. Demus, H. Demus and H. Zashcke, *Flussige Kristalle in Tabellen*, (VEN Deutscher Verlag für Grundstoffindustrie, Leipzig, 1974) p. 65.
15. S. C. Abrahams, *Quart. Rev.*, **10**, 407 (1956).
16. A. L. McClellan, *Tables of Experimental Dipole Moments*, (W. F. Freeman & Co., San Francisco, 1963) pp. 411-413.
17. A. J. Gordon and R. A. Ford, *The Chemists Companion*, (John Wiley & Sons, Inc., New York, 1972), pp. 84-87.
18. A. de Vries, Liquid Crystal Institute, Kent State University, Kent, Ohio, personal communication, 1980.
- 18a. A. Ekachai, A. de Vries, M. E. Neubert and N. Spielberg, submitted for publication to *J. Chem. Phys.*, 1980.
19. D. L. Johnson, Kent State University, Kent, Ohio, personal communication, 1980.
20. J. W. Goodby and G. W. Gray, *Mol. Cryst. Liq. Cryst.*, **48**, 127 (1978).
21. M. E. Neubert and L. J. Maurer, *Mol. Cryst. Liq. Cryst.*, **43**, 313 (1977).
22. N. A. P. Vaz, J. W. Doane and M. E. Neubert, submitted for publication in *Biochim. Biophys. Acta*, 1980.
23. J. A. Janik, Institute of Nuclear Physics, Krakow, Poland, personal communication, 1980.
24. L. Richter, D. Demus and H. Sackmann, *J. Phys. (Paris) Colloq.*, **37**, C3-41 (1976).
25. H. Sackmann, *J. Phys. (Paris) Colloq.*, **40**, C3-5 (1979).
26. E. M. Barrall II and J. F. Johnson in *Liquid Crystals and Plastic Crystals 2*, G. W. Gray and P. A. Winsor, eds. (Ellis Horwood Publisher, Chichester, England, 1974) Chapter 10.
27. E. M. Barrall II in *Liquid Crystals—The Fourth State of Matter*, F. D. Saeva, Ed. (Marcel Dekker, New York, NY, 1979) Chapter 9.
28. C. A. Schantz and D. L. Johnson, *Phys. Rev.*, **A 17**, 1504 (1978).
29. S. J. Majoros, D. J. Brisbin, D. L. Johnson and M. E. Neubert, *Phys. Rev.*, **A 20**, 1619 (1979).
30. K. C. Lim, J. T. Ho and M. E. Neubert, *Mol. Cryst. Liq. Cryst.*, **58**, 245 (1980).
31. P. Ukleja, M. Neubert and J. W. Doane, XIXth Congress Amper, Heidelberg, 209 (1976).
32. P. E. Cladis, D. Guillon, J. Stamatoff, D. Aadsen, W. P. Daniels, M. E. Neubert and R. F. Griffith, *Mol. Cryst. Liq. Cryst.*, **49**, 279 (1979).
33. F. J. Kahn, *Appl. Phys. Lett.*, **22**, 386 (1973).